Use of Computational and Synthetic Chemistry in Catalyst Design: A New Family of High-Activity Ethylene Polymerization Catalysts Based on Titanium Tris(amino)phosphinimide Complexes

Chad Beddie, Emily Hollink, Pingrong Wei, James Gauld, and Douglas W. Stephan*

Department of Chemistry and Biochemistry, University of Windsor, Windsor, Ontario, Canada, N9B3P4

Received June 22, 2004

DFT calculations of the mechanism of polymerization for the series of catalyst models derived from $CpTiMe_2(NPR_3)$ (R = Me, NH_2, H, Cl, F) demonstrate the critical role of ion pairing in determining the overall barrier to polymerization and suggest that electron-donating substituents reduce this barrier. Based on these results, a family of precatalysts of general formula $Cp'TiX_2(NP(NR_2)_3)$ (X = Cl, Me) were developed. This approach using computational methods to guide the synthetic efforts has afforded a new, readily accessible, and easily varied family of highly active ethylene polymerization catalysts based on titanium tris(amino)phosphinimide complexes.

Introduction

Since the discovery that zirconocene derivatives can act as single-site catalysts for olefin polymerization, efforts have been ongoing both in academic and in industrial labs to uncover alternative or modified catalyst systems. While many groups have targeted the control of polymer properties via judicious modification of zirconocene precursors, others have probed the viability of early metal complexes with alternative ancillary ligands as effective polymerization catalysts. In such efforts, a number of systems have drawn considerable attention. For example, in 1996, McConville and co-workers uncovered a nonmetallocene living polymerization catalyst (**A**), based on a bulky chelating diamide ligand.[1] A wide variety of other ligand modifications have been probed. Appreciable catalytic activities have been derived from titanium and zirconium complexes containing amido,[2] diamido,[3−8] bidentate aryloxide,[9−11] borollide,[12,13] boratabenzene,[14,15] pendant cyclopentadienyl borane,[16] trimethylene,[17] cyclopentadienylborate,[18] diketimine,[19] tropidinyl,[20] tridentate,[21] and macrocyclic ligands.[22] These and other efforts have been recently reviewed by Gibson and co-workers.[23,24] The "constrained geometry catalysts" (CGC) (**B**)[25−33] derived from Cp-amido ligand complexes have been

* To whom correspondence should be addressed. E-mail: stephan@uwindsor.ca.

(1) Scollard, J. D.; McConville, D. H. *J. Am. Chem. Soc.* **1996**, *118*, 10008−10009.
(2) Sinnema, P. J.; Okuda, J. *J. Organomet. Chem.* **2000**, *598*, 179−181.
(3) Lorber, C.; Donnadieu, B.; Choukroun, R. *Organometallics* **2000**, *19*, 1963−1966.
(4) Scollard, J. D.; McConville, D. H. *J. Am. Chem. Soc.* **1996**, *118*, 10008−10009.
(5) Scollard, J. D.; McConville, D. H.; Vittal, J. J. *Organometallics* **1995**, *14*, 8.
(6) Warren, T. H.; Schrock, R. R.; Davis, W. M. *Organometallics* **1998**, *17*, 308−321.
(7) Cloke, F. G. N.; Geldach, T. J.; Hitchcock, P. B.; Love, J. B. *J. Organomet. Chem.* **1996**, *506*, 343−345.
(8) Lee, C. H.; La, Y.-H.; Park, J. W. *Organometallics* **2000**, *19*, 344−351.
(9) Nomura, K.; Naga, N.; Miki, M.; Yanagi, K.; Imai, A. *Organometallics* **1998**, *17*, 2152−2154.
(10) Tsukahara, T.; Swenson, D. C.; Jordan, R. F. *Organometallics* **1997**, *16*, 3303−3313.
(11) Van Der Linden, A.; Schaverien, C. J.; Meijboom, N.; Ganter, C.; Orpen, A. G. *J. Am. Chem. Soc.* **1995**, *117*, 3008−3021.
(12) Bazan, G. C.; Schaefer, W. P.; Bercaw, J. E. *Organometallics* **1993**, *12*, 2126.
(13) Bazan, G. C.; Donnelly, S. J.; Ridriguez, G. *J. Am. Chem. Soc.* **1995**, *117*, 2671−2672.
(14) Bazan, G. C.; Rodriguez, G.; Ashe, A. J., III; Al-Ahmad, S.; Muller, C. *J. Am. Chem. Soc.* **1996**, *118*, 2291−2292.
(15) Bazan, G. C.; Rodriguez, G. *Organometallics* **1997**, *16*, 2492−2494.
(16) Spence, R. E. v. H.; Piers, W. E. *Organometallics* **1995**, *14*, 4617−4624.
(17) Rodriguez, G.; Bazan, G. C. *J. Am. Chem. Soc.* **1997**, *119*, 343−352.
(18) Sun, Y.; Spence, R. E. v. H.; Piers, W. E.; Parvez, M.; Yap, G. P. A. *J. Am. Chem. Soc.* **1997**, *119*, 5132−5143.
(19) Vollmerhaus, R.; Rahim, M.; Tomaszewski, R.; Xin, S.; Taylor, N. J.; Collins, S. *Organometallics* **2000**, *19*, 2161−2169.
(20) Skoog, S. J.; Mateo, C.; Lavoie, G. G.; Hollander, F. J.; Bergman, R. G. *Organometallics* **2000**, *19*, 1406−1421.
(21) Okuda, J.; Eberle, T.; Spaniol, T. P.; Piquet-Faure, V. *J. Organomet. Chem.* **2000**, *591*, 127−137.
(22) Fokken, S.; Spaniol, T. P.; Kang, H.-C.; Massa, W.; Okuda, J. *Organometallics* **1996**, *15*, 5069−5072.
(23) Gibson, V. C.; Spitzmesser, S. K. *Chem. Rev.* **2003**, *103*, 283−315.
(24) Britovsek, G. J. P.; Gibson, V. C.; Wass, D. F. *Angew. Chem., Int. Ed.* **1999**, *38*, 428−447.
(25) Shapiro, P. J.; Bunel, E.; Schaefer, W. P.; Bercaw, J. E. *Organometallics* **1990**, *9*, 867−869.
(26) Chen, Y.-X.; Marks, T. J. *Organometallics* **1997**, *16*, 3649−3657.
(27) Tian, S.; Arredondo, V. M.; Stern, C. L.; Marks, T. J. *Organometallics* **1999**, *18*, 2568−2570.
(28) Deck, P. A.; Beswick, C. L.; Marks, T. J. *J. Am. Chem. Soc.* **1998**, *120*, 1772−1784.
(29) Woo, T. K.; Margl, P. M.; Lohrenz, J. C. W.; Blochl, P. E.; Ziegler, T. *J. Am. Chem. Soc.* **1996**, *118*, 13021−13030.
(30) Shapiro, P. J.; Cotter, W. D.; Schaefer, W. P.; Labinger, J. A.; Bercaw, J. E. *J. Am. Chem. Soc.* **1994**, *116*, 4623−4640.
(31) Devore, D. D.; Timmers, F. J.; Hasha, D. L.; Rosen, R. K.; Marks, T. J.; Deck, P. A.; Stern, C. L. *Organometallics* **1995**, *14*, 3132−3134.
(32) Lindsay, K. F. *Mod. Plast.* **1993**, 82.

10.1021/om049545i CCC: $27.50
Publication on Web 09/25/2004

Scheme 1. Examples of Non-metallocene Catalyst Precursors

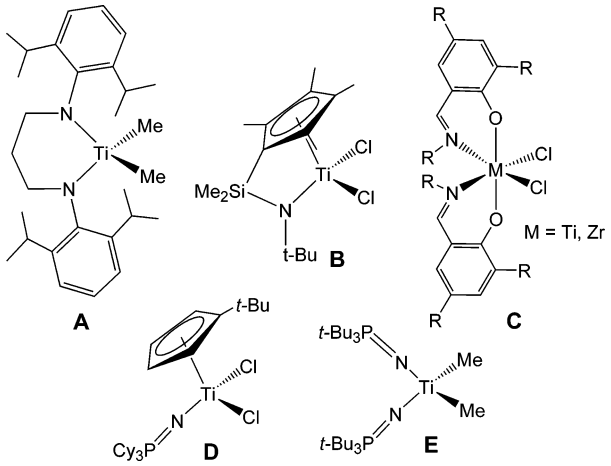

commercialized by Dow and Exxon. More recently, Fujita and co-workers at Mitsui Chemicals have developed the so-called "FI catalysts" (*Fenokishi-Imin*), which are phenoxy-imine ligand complexes of zirconium and titanium (**C**).[34,35] In our own efforts to develop nonmetallocene catalyst systems, we have focused on Ti-phosphinimide ligand complexes. While small substituents on the phosphinimide ligands prompt unique deactivation pathways, including formation of Ti(IV) dications[36] and multiple C−H activation processes,[37−39] sterically demanding phosphinimide complexes such as (C_5H_4t-Bu)$TiCl_2NPCy_3$ (**D**) or $TiMe_2(NPt\text{-}Bu_3)_2$ (**E**) afford highly active catalysts that sustain activity under industrially relevant conditions.[40−42] Further studies involving a variety of sterically demanding phosphinimide ligands have revealed the complexity of catalyst design issues for these ancillary ligands.[43,44] The nature of desirable electronic features is also unclear. Preliminary studies using a series of substituted triphenylphosphinimide Ti-precatalysts demonstrated increased activity when electron-donating substituents were incorporated; however these catalysts operate in a rather low activity regime.[42] Nonetheless, a recent study of a related CpTi-ketimide system showed that incorporation of bulky electron-donating amides resulted in improved catalyst performance.[45] While computational studies of polymerization catalysts have for the most part focused on metallocene[46−70] and constrained geometry-based catalysts,[48,49,51,57,60,62,71,72] group 4 phosphinimide catalysts have only recently been investigated by Ziegler and co-workers.[58,59] While these experimental and theoretical investigations have illuminated various aspects of successful olefin polymerization catalyst targets, in general, the discovery of high-activity nonmetallocene catalysts has, for the most part, been the product of serendipity. In this article, we employ computational methods to provide guidance for the synthetic chemistry efforts of new phosphinimide catalysts. The energetics of model reactions of phosphinimide catalysts with ethylene, resulting in two consecutive insertions, are computed as a function of the phosphinimide substituents using density functional theory. These results are used together with judicious synthetic strategies to uncover a new family of readily accessible, highly active ethylene polymerization catalysts based on titanium tris(amino)phosphinimide complexes.

Experimental Section

General Data. All preparations were done under an atmosphere of dry, O_2-free N_2 employing both Schlenk line techniques and an MBraun inert atmosphere glovebox. Sol-

(33) Stevens, J. C. In *Catalyst Design for Taylor-made Polyolefins, Studies in Surface Science and Catalysis*; Soga, K., Terano, M., Eds.; Elsevier: Amsterdam, 1994; Vol. 89, pp 277−284.
(34) Makio, H.; Kashiwa, N.; Fujita, T. *Adv. Synth. Catal.* **2002**, *344*, 477−493.
(35) Mitani, M.; Nakano, T.; Fujita, T. *Chem. Eur. J.* **2003**, *9*, 2396−2403.
(36) Guerin, F.; Stephan, D. W. *Angew. Chem., Int. Ed.* **2000**, *39*, 1298−1300.
(37) Kickham, J. E.; Guerin, F.; Stephan, D. W. *J. Am. Chem. Soc.* **2002**, *124*, 11486−11494.
(38) Kickham, J. E.; Guerin, F.; Stewart, J. C.; Stephan, D. W. *Angew. Chem., Int. Ed.* **2000**, *39*, 3263−3266.
(39) Kickham, J. E.; Guerin, F.; Stewart, J. C.; Urbanska, E.; Stephan, D. W. *Organometallics* **2001**, *20*, 1175−1182.
(40) Stephan, D. W.; Stewart, J. C.; Guerin, F.; Spence, R. E. v. H.; Xu, W.; Harrison, D. G. *Organometallics* **1999**, *18*, 1116−1118.
(41) Stephan, D. W.; Guerin, F.; Spence, R. E. v. H.; Koch, L.; Gao, X.; Brown, S. J.; Swabey, J. W.; Wang, Q.; Xu, W.; Zoricak, P.; Harrison, D. G. *Organometallics* **1999**, *18*, 2046−2048.
(42) Stephan, D. W.; Stewart, J. C.; Guerin, F.; Courtenay, S.; Kickham, J.; Hollink, E.; Beddie, C.; Hoskin, A.; Graham, T.; Wei, P.; Spence, R. E. v. H.; Xu, W.; Koch, L.; Gao, X.; Harrison, D. G. *Organometallics* **2003**, *22*, 1937−1947.
(43) Carraz, C.-A.; Stephan, D. W. *Organometallics* **2000**, *19*, 3791−3796.
(44) Yue, N. L. S.; Stephan, D. W. *Organometallics* **2001**, *20*, 2303−2308.
(45) Kretschmer, W. P.; Dijkhuis, C.; Meetsma, A.; Hessen, B.; Teuben, J. H. *Chem. Commun.* **2002**, 608−609.
(46) Fusco, R.; Longo, L.; Masi, F.; Garbassi, F. *Macromolecules* **1997**, *30*, 7673−7685.
(47) Fusco, R.; Longo, L.; Proto, A.; Masi, F.; Garbassi, F. *Macromol. Rapid Commun.* **1998**, *19*, 257−262.
(48) Lanza, G.; Fragala, I. L.; Marks, T. J. *J. Am. Chem. Soc.* **1998**, *120*, 8257−8258.
(49) Lanza, G.; Fragala, I. L. *Top. Catal.* **1999**, *7*, 45−60.
(50) Rappe, A. K.; Skiff, W. M.; Casewit, C. J. *Chem. Rev.* **2000**, *100*, 1435−1456.
(51) Lanza, G.; Fragala, I. L.; Marks, T. J. *J. Am. Chem. Soc.* **2000**, *122*, 12764−12777.
(52) Vanka, K.; Chan, M. S. W.; Pye, C. C.; Ziegler, T. *Organometallics* **2000**, *19*, 1841−1849.
(53) Braga, D.; Grepioni, F.; Tedesco, E.; Calhorda, M. J. *Z. Anorg. Allg. Chem.* **2000**, *626*, 462−470.
(54) Chan, M. S. W.; Ziegler, T. *Organometallics* **2000**, *19*, 5182−5189.
(55) Nifant'ev, I. E.; Ustynyuk, L. Y.; Laikov, D. N. *Organometallics* **2001**, *20*, 5375−5393.
(56) Vanka, K.; Ziegler, T. *Organometallics* **2001**, *20*, 905−913.
(57) Lanza, G.; Fragala, I. L.; Marks, T. J. *Organometallics* **2002**, *21*, 5594−5612.
(58) Xu, Z.; Vanka, K.; Firman, T.; Michalak, A.; Zurek, E.; Zhu, C.; Ziegler, T. *Organometallics* **2002**, *21*, 2444−2453.
(59) Vanka, K.; Xu, Z.; Ziegler, T. *Isr. J. Chem.* **2003**, *42*, 403−415.
(60) Woo, T. K.; Fan, L.; Ziegler, T. *Organometallics* **1994**, *13*, 2252−2261.
(61) Yoshida, T.; Koga, N.; Morokuma, K. *Organometallics* **1995**, *14*, 746−758.
(62) Woo, T. K.; Margl, P. M.; Ziegler, T.; Bloechl, P. E. *Organometallics* **1997**, *16*, 3454−3468.
(63) Margl, P.; Deng, L.; Ziegler, T. *J. Am. Chem. Soc.* **1999**, *121*, 154−162.
(64) Talarico, G.; Blok, A. N. J.; Woo, T. K.; Cavallo, L. *Organometallics* **2002**, *21*, 4939−4949.
(65) Bierwagen, E. P.; Bercaw, J. E.; Goddard, W. A., III. *J. Am. Chem. Soc.* **1994**, *116*, 1481−1489.
(66) Lohrenz, J. C. W.; Woo, T. K.; Fan, L.; Harrison, D.; Margl, P.; Ziegler, T. *Polym. Mater. Sci. Eng.* **1996**, *74*, 391−392.
(67) Thorshaug, K.; Stovneng, J. A.; Rytter, E.; Ystenes, M. *Macromolecules* **1998**, *31*, 7149−7165.
(68) Margl, P. M.; Woo, T. K.; Ziegler, T. *Organometallics* **1998**, *17*, 4997−5002.
(69) Chan, M. S. W.; Vanka, K.; Pye, C. C.; Ziegler, T. *Organometallics* **1999**, *18*, 4624−4636.
(70) Lanza, G.; Fragala, I. L.; Marks, T. J. *Organometallics* **2001**, *20*, 4006−4017.

vents were purified employing a Grubbs type solvent purification system manufactured by Innovative Technology. All organic reagents were purified by conventional methods. ^{1}H, ^{31}P{^{1}H}, and ^{13}C{^{1}H} NMR spectra were recorded on Bruker Avance-300 and -500 spectrometers. All spectra were recorded in C_6D_6 at 25 °C unless otherwise noted. Trace amounts of protonated solvents were used as references, and chemical shifts are reported relative to $SiMe_4$. The ^{31}P{^{1}H} NMR spectra were referenced to external 85% H_3PO_4. Combustion analyses were done in-house employing a Perkin-Elmer CHN analyzer. Me_3SiN_3, $P(NMe_2)_3$ (**1**), and $P(NEt_2)_3$ (**2**) were purchased from Aldrich Chemical Co. Cp*$TiCl_3$ was purchased from Strem Chemical Co., and P(N*n*-$Pr_2)_3$ (**3**) was purchased from Lancaster Chemicals. $B(C_6F_5)_3$ and MAO were generously donated by NOVA Chemicals Corporation. $CpTiCl_3$,[73] P(N*n*-$Bu_2)_3$ (**4**),[74] P(*N*-3-methylindolyl)$_3$ (**7**),[75] $Me_3SiNP(NMe_2)_3$ (**8**),[76] $Me_3SiNP(NEt_2)_3$ (**9**),[77] $Me_3SiNP(N$*n*-$Bu_2)_3$ (**11**),[78] and $CpTiCl_2NP(NMe_2)_3$ (**15**)[79] were prepared via literature methods.

Synthesis of P(N*i*-PrMe)$_3$ (5).[80] To a solution of PCl_3 (2.07 mL, 23.7 mmol) and NEt_3 (11.6 mL, 83.2 mmol) in ether (300 mL), cooled to −78 °C, was slowly added HN*i*-PrMe (8.65 mL, 83.1 mmoL) via syringe. The resulting white slurry was allowed to warm to room temperature over a period of 1 h. The slurry was filtered via a filter cannula to a produce a clear, yellow solution. The white solid was washed with 3 × 75 mL of ether, and the washings were transferred through the filter cannula and added to the original filtrate. The solvent was partially removed under vacuum to produce a white suspension. The white suspension was filtered through Celite, and the residual white solid was washed with 10 mL of ether. The solvent and excess HN(*i*-Pr)(Me) were removed from the filtrate under vacuum to produce an oil, which was purified by vacuum distillation, yielding a clear colorless liquid. **3**: yield 3.17 g, 12.8 mmol, 54%. ^{31}P{^{1}H} NMR: δ 119.7. ^{1}H NMR: δ 3.58 (d of sept, 3H, $^3J_{P-H}$ = 10 Hz,$^3J_{H-H}$ = 7 Hz CHMe$_2$), 2.34 (d, 9H, $^3J_{P-H}$ = 6 Hz, NMe), 1.09 (d, 18H, $^3J_{H-H}$ = 7 Hz, CHMe$_2$). ^{13}C{^{1}H} NMR: δ 49.2 (d, $^2J_{PC}$ = 36 Hz, CHMe$_2$), 26.5 (d, $^2J_{PC}$ = 5 Hz, NMe), 21.1 (d, $^3J_{PC}$ = 4 Hz, CHMe$_2$).

Synthesis of P(NEtPh)$_3$ (6).[81] To a solution of PCl_3 (5.0 mL, 57.3 mmol) and NEt_3 (28.0 mL, 201 mmol) in toluene (400 mL) cooled to 0 °C was slowly added HNEtPh (25.3 mL, 187 mmol) via syringe. The white suspension was heated at refluxing temperature for 12 h. The mixture was cooled to room temperature and then filtered through a cannula filter to produce a yellow solution. The volatiles were removed under vacuum to produce a yellow solid. ^{31}P{^{1}H} NMR revealed the presence of two products; therefore 300 mL of toluene, NEt_3 (16.0 mL, 115 mmol), and HNEtPh (7.2 mL, 57.2 mmol) were added. The mixture was heated at refluxing temperature for an additional 12 h. The mixture was cooled to room temperature and then filtered through a cannula filter to produce a yellow solution. The volume of the solution was reduced to ∼50 mL under vacuum, which resulted in the precipitation of a white solid. In the glovebox the slurry was filtered and a white solid collected in the filter frit. The solid was extracted with ∼250 mL of toluene. The solvent was removed from the filtrate under vacuum to produce **6** as a white solid. Yield: 12.14 g, 31.0 mmol, 54%. ^{31}P{^{1}H} NMR: δ 110.4. ^{1}H NMR: δ 7.17−7.11 (m, 12H, NPh), 6.86 (tt, 3H, $^3J_{H-H}$ = 7 Hz, $^4J_{H-H}$ = 2 Hz, NPh), 3.37 (dq, 6H, $^3J_{P-H}$ = 3 Hz, $^3J_{H-H}$ = 7 Hz, NCH$_2$Me), 0.94 (t, 9H, $^3J_{H-H}$ = 7 Hz, NCH$_2$Me). ^{13}C{^{1}H} NMR: δ 147.4 (d, $^2J_{P-C}$ = 22 Hz, NPh (*ipso*)), 129.6 (NPh), 122.1 (NPh), 121.9 (NPh), 40.9 (NCH$_2$Me), 14.2 (NCH$_2$Me). Anal. Found: C, 73.99; H, 7.87; N, 10.74. Calcd: C, 73.63; H, 7.72; N, 10.73. X-ray quality crystals were obtained by slow evaporation of toluene.

Syntheses of Me$_3$SiNP(NMe$_2$)$_3$ (8),[76] Me$_3$SiNP(NEt$_2$)$_3$ (9),[77] Me$_3$SiNP(N*n*-Pr$_2$)$_3$ (10), Me$_3$SiNP(N*n*-Bu$_2$)$_3$ (11),[78] Me$_3$SiNP(N*i*-PrMe)$_3$ (12), and Me$_3$SiNP(NEtPh)$_3$ (13).[78] These compounds were prepared in a similar manner, and thus only one synthesis is detailed. To a solution of $P(NMe_2)_3$ (3.00 mL, 16.5 mmol) in toluene (30 mL) was added Me_3SiN_3 (3.29 mL, 24.8 mmol). The resulting solution was heated at refluxing temperature for 12 h. The solvent and excess Me_3SiN_3 were removed under vacuum, resulting in a crude oil that was purified by vacuum distillation to give a clear, colorless oil. **8**:[76] Yield: 3.05 g, 12.2 mmol, 74%. ^{31}P{^{1}H} NMR: δ 14.9. ^{1}H NMR: δ 2.40 (d, 18H, $^3J_{P-H}$ = 10 Hz, NMe$_2$), 0.39 (s, 9H, SiMe$_3$). ^{13}C{^{1}H} NMR: δ 37.6 (d, $^2J_{PC}$ = 3 Hz, NMe$_2$), 5.1 (SiMe$_3$). **9**:[77] Yield: 2.80 g, 8.38 mmol, 68%. ^{31}P{^{1}H} NMR: δ 9.7. ^{1}H NMR: δ 2.94 (dq, 12H, $^3J_{P-H}$ = 10 Hz, $^3J_{H-H}$ = 7 Hz, NCH$_2$), 0.99 (t, 18H, $^3J_{H-H}$ = 7 Hz, (CH$_2$Me)), 0.39 (s, 9H, SiMe$_3$). ^{13}C{^{1}H} NMR: δ 40.0 (d, $^2J_{PC}$ = 5 Hz, NCH$_2$), 14.7 (d, $^3J_{PC}$ = 3 Hz, CH$_2$Me), 4.9 (SiMe$_3$). **10**: Yield: 2.25 g, 5.38 mmol, 89%. ^{31}P{^{1}H} NMR: δ 10.3. ^{1}H NMR: δ 2.89 (m, 12H, N(CH$_2$)), 1.53 (m, 12H, CH$_2$CH$_2$Me), 0.84 (t, 18H, $^3J_{H-H}$ = 7 Hz, CH$_2$Me), 0.41 (s, 9H, SiMe$_3$). ^{13}C{^{1}H} NMR: δ 49.2 (d, $^2J_{P-C}$ = 4 Hz, NCH$_2$), 23.0 (d, $^3J_{P-C}$ = 2 Hz, CH$_2$CH$_2$Me), 12.2 (s, CH$_2$Me), 5.0 (s, SiMe$_3$). Anal. Found: C, 59.33; H, 11.39; N, 14.65 Calcd: C, 60.24; H, 12.28; N, 13.38. **11**:[78] Yield: 2.19 g, 4.35 mmol, 91%. ^{31}P{^{1}H} NMR: δ 10.9 (s). ^{1}H NMR: δ 3.02 (dt, 12H, $^3J_{P-H}$ = 10 Hz,$^3J_{H-H}$ = 8 Hz NCH$_2$), 1.59 (m, 12H, CH$_2$-CH$_2$CH$_2$), 1.28 (pseudo sextet, 12H, $^3J_{H-H}$ = 7 Hz, CH$_2$CH$_2$-Me), 0.98 (t, 18H, $^3J_{H-H}$ = 7 Hz, CH$_2$Me), 0.43 (s, 9H, SiMe$_3$). ^{13}C{^{1}H} NMR: δ 47.1 (d, $^2J_{P-C}$ = 4 Hz, NCH$_2$), 32.1 (d, $^3J_{P-C}$ = 2 Hz, CH$_2$CH$_2$CH$_2$), 21.5 (s, CH$_2$CH$_2$Me), 14.7 (s, CH$_2$Me), 5.1 (s, SiMe$_3$). **12**: Yield: 2.52 g, 7.54 mmol, 68%. ^{31}P{^{1}H} NMR: δ 10.6. ^{1}H NMR: δ 4.00 (d(sept), 3H, $^3J_{P-H}$ = 10 Hz,$^3J_{H-H}$ = 7 Hz, CHMe$_2$), 2.25 (d, 9H, $^3J_{P-H}$ = 10 Hz, NMe), 1.01 (d, 18H, $^3J_{H-H}$ = 7 Hz, CHMe$_2$), 0.36 (s, 9H, SiMe$_3$). ^{13}C-{^{1}H} NMR: δ 46.1 (d, $^2J_{P-C}$ = 5 Hz, CHMe$_2$), 26.7 (d, $^2J_{P-C}$ = 4 Hz, NMe), 20.7 (CHMe$_2$), 4.9 (SiMe$_3$). Anal. Found: C, 53.21; H, 11.30; N, 17.16. Calcd: C, 53.85; H, 11.75; N, 16.75. **13**: Yield: 3.56 g, 7.43 mmol, 90%. ^{31}P{^{1}H} NMR: δ −5.8. ^{1}H NMR: δ 7.21 (d, 6H, $^3J_{H-H}$ = 8 Hz, NPh), 7.16 (t, 6H, $^3J_{H-H}$ = 8 Hz, NPh), 7.00 (t, 3H, $^3J_{H-H}$ = 8 Hz, NPh), 3.38 (dq, 6H, $^3J_{P-H}$ = 7 Hz, $^3J_{H-H}$ = 7 Hz, NCH$_2$Me), 0.79 (t, 9H, $^3J_{H-H}$ = 7 Hz, NCH$_2$Me), 0.04 (s, 9H, SiMe$_3$). ^{13}C{^{1}H} NMR: δ 144.9 (s, NPh (*ipso*)), 129.9 (d, $^3J_{P-C}$ = 3 Hz, NPh), 128.6 (NPh), 125.7 (NPh), 46.9 (NCH$_2$Me), 14.5 (NCH$_2$Me), 3.9 (SiMe$_3$).

Syntheses of Cp′TiCl$_2$(NP(NR$_2$)$_3$) (Cp′ = Cp, R = Me 15,[79] Et 16, Pr 17, Bu 18, R$_2$ = *i*-PrMe 19, EtPh 20; Cp′ = Cp*, R = Me 21, Et 22, Pr 23, Bu 24, R$_2$ = *i*-PrMe 25, EtPh 26). These compounds were prepared in a similar manner, and thus only one synthesis is detailed. To a yellow solution of $CpTiCl_3$ (0.400 g, 1.82 mmol) in toluene (30 mL) was added a solution of $Me_3SiNP(NMe_2)_3$ (**8**) (0.480 g, 1.92 mmol) in toluene (20 mL). The resulting solution was stirred at room temperature for 12 h. The volume of the solution was reduced under vacuum to cause the formation of a yellow solid. The solid was washed with hexanes (3 × 5 mL) and dried under vacuum to give a yellow solid. **15**: Yield: 0.630 g, 1.74 mmol, 96%. ^{31}P-{^{1}H} NMR: δ 5.6. ^{1}H NMR: δ 6.44 (s, 5H, Cp), 2.24 (d, 18H, $^3J_{P-H}$ = 10 Hz, NMe$_2$). ^{13}C{^{1}H} NMR: δ 115.4 (Cp), 37.1 (d,

(71) Woo, T. K.; Margl, P. M.; Lohrenz, J. C. W.; Bloechl, P. E.; Ziegler, T. *J. Am. Chem. Soc.* **1996**, *118*, 13021−13030.
(72) Xu, Z.; Vanka, K.; Ziegler, T. *Organometallics* **2004**, *23*, 104−116.
(73) Gorsich, R. D. *J. Am. Chem. Soc.* **1960**, *82*, 4211−4214.
(74) Vogt, H.; Wulff-Molder, D.; Ritschl, F.; Mucke, M.; Skrabei, U.; Meisel, M. *Z. Anorg. Allg. Chem.* **1999**, *625*, 1025−1027.
(75) Barnard, T. S.; Mason, M. R. *Organometallics* **2001**, *20*, 206−214.
(76) Schlak, O.; Stadelmann, W.; Stelzer, O.; Schmutzler, R. *Z. Anorg. Allg. Chem.* **1976**, *419*, 275−282.
(77) Flindt, E. P.; Rose, H.; Marsmann, H. C. *Z. Anorg. Allg. Chem.* **1977**, *430*, 155−160.
(78) Marchenko, A. P.; Koidan, G. N.; Pinchuk, A. M.; Kirsanov, A. V. *Z. Obsh. Khim.* **1984**, *54*, 1774−1782.
(79) Spence, R. E. V. H.; Koch, L.; Jeremic, D.; Brown, S. J. (Nova Chemicals (International) S.A., Switz.) PCT Int. Appl.; WO, 2000, 32 pp.
(80) Nagato, N.; Ogawa, M.; Naito, T. (Showa Denko K. K.) Jpn. Kokai Tokkyo Koho; Jp, 1973; 6 pp.
(81) Marchenko, A. P.; Pinchuk, A. M.; Feshchenko, N. G. *Z. Obsh. Khim.* **1973**, *43*, 1900−1903.

$^2J_{PC}$ = 4 Hz, NMe_2). Anal. Found: C, 36.31; H, 6.77; N, 15.39. Calcd: C, 36.59; H, 6.42; N, 15.52. **16**: Yield: 1.28 g, 2.88 mmol, 95%. $^{31}P\{^1H\}$ δ NMR: 3.4. ^1H NMR: δ 6.48 (s, 5H, Cp), 2.82 (dq, 12H, $^3J_{P-H}$ = 11 Hz, $^3J_{H-H}$ = 7 Hz, CH_2Me), 0.90 (t, 18H, $^3J_{H-H}$ = 7 Hz, CH_2Me). $^{13}C\{^1H\}$ NMR: δ 115.3 (Cp), 39.9 (d, $^2J_{P-C}$ = 5 Hz, CH_2Me), 14.2 (d, $^3J_{P-C}$ = 3 Hz, CH_2Me). Anal. Found: C, 45.39; H, 7.99; N, 12.59. Calcd: C, 45.86; H, 7.92; N, 12.58. **17**: Yield: 0.234 g, 0.442 mmol, 96%. $^{31}P\{^1H\}$ NMR: 3.8. ^1H NMR: 6.50 (s, 5H, Cp), 2.85 (m, 12H, CH_2CH_2Me), 1.48 (m, 12H, CH_2CH_2Me), 0.82 (t, 18H, $^3J_{H-H}$ = 7 Hz, CH_2Me). $^{13}C\{^1H\}$ NMR: 115.3 (Cp), 48.5 (d, $^2J_{P-C}$ = 4 Hz, CH_2CH_2Me), 22.5 (d, $^3J_{P-C}$ = 3 Hz, CH_2CH_2Me), 12.0 (s, CH_2Me). Anal. Found: C, 51.42; H, 8.96; N, 10.64. Calcd: C, 52.18; H, 8.95; N, 10.58. **18**: Yield: 0.277 g, 0.451 mmol, 97%. $^{31}P\{^1H\}$ NMR: δ 4.5. ^1H NMR: δ 6.53 (s, 5H, Cp), 3.00 (m, 12H, $CH_2CH_2CH_2$), 1.57 (m, 12H, $CH_2CH_2CH_2Me$), 1.28 (pseudo sextet, 12H, $^3J_{H-H}$ = 7 Hz, $CH_2CH_2CH_2Me$), 0.94 (t, 18H, $^3J_{H-H}$ = 7 Hz, CH_2Me). $^{13}C\{^1H\}$ NMR: δ 115.3 (Cp), 46.6 (d, $^2J_{P-C}$ = 4 Hz, NCH_2), 31.5 (d, $^3J_{P-C}$ = 3 Hz, $CH_2CH_2CH_2$), 21.2 (s, CH_2CH_2Me), 14.6 (s, CH_2Me). Anal. Found: C, 55.83; H, 9.23; N, 8.23. Calcd: C, 56.77; H, 9.69; N, 9.13. **19**: Yield: 1.15 g, 2.59 mmol, 86%. $^{31}P\{^1H\}$ NMR: δ 3.4. ^1H NMR: δ 6.47 (s, 5H, Cp), 4.04 (d(sept), 3H, $^3J_{P-H}$ = 10 Hz,$^3J_{H-H}$ = 7 Hz $CHMe_2$), 2.07 (d, 9H, $^3J_{P-H}$ = 10 Hz, NMe), 0.96 (d, 18H, $^3J_{H-H}$ = 7 Hz, $CHMe_2$). $^{13}C\{^1H\}$ NMR: δ 115.2 (Cp), 46.9 (d, $^2J_{P-C}$ = 5 Hz, $CHMe_2$), 26.6 (d, $^2J_{P-C}$ = 4 Hz, NMe), 20.7 (d, $^3J_{P-C}$ = 3 Hz, $CHMe_2$). Anal. Found: C, 45.56; H, 8.14; N, 12.45. Calcd: C, 45.86; H, 7.92; N, 12.58. X-ray quality crystals were obtained from slow evaporation of a toluene/hexanes solution. **20**: Yield: 0.946 g, 1.61 mmol, 88%. $^{31}P\{^1H\}$ NMR: δ −11.1. ^1H NMR: δ 7.21 (d, 6H, $^3J_{H-H}$ = 8 Hz, NPh (*ortho*)), 7.13 (pseudo t, 6H, $^3J_{H-H}$ = 8 Hz, NPh (*meta*)), 6.97 (t, 3H, $^3J_{H-H}$ = 8 Hz, NPh (*para*)), 6.03 (s, 5H, Cp), 3.38 (dq, 6H, $^3J_{P-H}$ = 7 Hz, $^3J_{H-H}$ = 7 Hz, NCH_2Me), 0.66 (t, 9H, $^3J_{H-H}$ = 7 Hz, NCH_2Me). $^{13}C\{^1H\}$ NMR: δ 141.9 (d, $^2J_{P-C}$ = 4 Hz, NPh (*ipso*)), 130.9 (d, $^3J_{P-C}$ = 3 Hz, NPh (*ortho*)), 129.6 (s, NPh (*meta*)), 127.2 (s, NPh (*para*)), 116.2 (s. Cp), 46.8 (d, $^2J_{P-C}$ = 4 Hz, NCH_2Me), 14.0 (d, $^3J_{P-C}$ = 4 Hz, NCH_2Me). Anal. Found: C, 58.72; H, 6.08; N, 9.61. Calcd: C, 59.10; H, 5.99; N, 9.51. **21**: Yield: 0.505 g, 1.17 mmol, 68%. $^{31}P\{^1H\}$ NMR: 6.1 (s). ^1H NMR: 2.35 (d, 18H, $^3J_{P-H}$ = 10 Hz, NMe_2), 2.21 (s, 15H, Cp*). $^{13}C\{^1H\}$ NMR: 126.1 (Cp*), 37.5 (d, $^2J_{P-C}$ = 4 Hz, NMe_2), 13.4 (Cp*). Anal. Found: C, 44.33; H, 7.57; N, 13.05. Calcd: C, 44.57; H, 7.71; N, 12.99. X-ray quality crystals were obtained from slow evaporation of a toluene/hexanes solution. **22**: Yield: 0.586 g, 1.14 mmol, 57%. $^{31}P\{^1H\}$ NMR: δ 5.6. ^1H NMR: δ 2.97 (dq, 12H, $^3J_{P-H}$ = 11 Hz, $^3J_{H-H}$ = 7 Hz, NCH_2Me), 2.22 (s, 15H, Cp*), 0.95 (t, 18H, $^3J_{H-H}$ = 7 Hz, CH_2Me). $^{13}C\{^1H\}$ NMR: δ 125.7 (Cp*), 39.8 (d, $^2J_{P-C}$ = 5 Hz, CH_2Me), 14.1 (d, $^3J_{P-C}$ = 3 Hz, CH_2Me), 13.4 (Cp*). Anal. Found: C, 50.81; H, 8.60; N, 11.06. Calcd: C, 51.27; H, 8.80; N, 10.87. X-ray quality crystals were obtained from slow evaporation of a toluene/hexanes solution. **23**: Yield: 0.574 g, 0.957 mmol, 96%. $^{31}P\{^1H\}$ NMR: δ 5.0.^1H NMR: δ 2.99 (m, 12H, NCH_2), 2.24 (s, 15H, Cp*), 1.52 (m, 12H, CH_2CH_2Me), 0.85 (t, 18H, $^3J_{H-H}$ = 7 Hz, CH_2Me).$^{13}C\{^1H\}$ NMR: δ 125.8 (Cp*), 48.4 (NCH_2), 22.1 (CH_2CH_2Me), 13.5 (Cp*), 12.0 (CH_2Me). Anal. Found: C, 55.15; H, 9.41; N, 9.27. Calcd: C, 56.09; H, 9.58; N, 9.35. **24**: Yield: 0.670 g, 0.980 mmol, 91%. $^{31}P\{^1H\}$ NMR: δ 5.4. ^1H NMR: δ 3.00 (m, 12H, NCH_2CH_2), 2.25 (s, 15H, Cp*), 1.61 (m, 12H, $CH_2CH_2CH_2$), 1.32 (pseudo sextet, 12H, $^3J_{H-H}$ = 7 Hz, CH_2CH_2Me), 0.96 (t, 18H, $^3J_{H-H}$ = 7 Hz, CH_2Me). $^{13}C\{^1H\}$ NMR: δ 125.8 (Cp*), 46.4 (d, $^2J_{P-C}$ = 4 Hz, NCH_2), 31.1 (d, $^3J_{P-C}$ = 3 Hz, $CH_2CH_2CH_2$), 21.3 (CH_2CH_2Me), 14.7 (CH_2Me), 13.5 (Cp*). Anal. Found: C, 59.50; H, 10.51; N, 8.18. Calcd: C, 59.73; H, 10.17; N, 8.19. **25**: Yield: 0.874 g, 1.70 mmol, 70%. $^{31}P\{^1H\}$ NMR: δ 4.4. ^1H NMR: δ 3.99 (d(sept), 3H, $^3J_{P-H}$ = 10 Hz,$^3J_{H-H}$ = 7 Hz $CHMe_2$), 2.22 (d, 9H, $^3J_{P-H}$ = 11 Hz, NMe), 2.21 (s, 15H, Cp*), 1.01 (d, 18H, $^3J_{H-H}$ = 6.7 Hz, $CHMe_2$). $^{13}C\{^1H\}$ NMR: δ 125.7 (Cp*), 46.7 (d, $^2J_{P-C}$ = 5 Hz, $CHMe_2$), 27.0 (d, $^2J_{P-C}$ = 4 Hz, NMe), 20.8 (d, $^3J_{P-C}$ = 3 Hz, $CHMe_2$), 13.4 (Cp*). Anal. Found: C, 51.47; H, 9.14; N, 10.85. Calcd: C, 51.27; H, 8.80; N, 10.87. **26**: Yield 0.786 g, 1.19 mmol, 85%. $^{31}P\{^1H\}$ NMR: δ −5.9. ^1H NMR: δ 7.16 (d, 6H, partially obscured by C_6D_6, NPh (*ortho*)), 7.09 (pseudo t, 6H, $^3J_{H-H}$ = 8 Hz, NPh (*meta*)), 6.96 (t, 3H, $^3J_{H-H}$ = 7 Hz, NPh (*para*)), 3.62 (dq, 6H, $^3J_{P-H}$ = 7 Hz, $^3J_{H-H}$ = 7 Hz, NCH_2Me), 2.15 (s, 15H, Cp*), 0.57 (t, 9H, $^3J_{H-H}$ = 7 Hz, NCH_2Me). $^{13}C\{^1H\}$ NMR: δ 142.5 (NPh (*ipso*)), 131.0 (d, $^3J_{P-C}$ = 3 Hz, NPh (*ortho*)), 129.4 (NPh (*meta*)), 126.9 (s, Cp*), 126.7 (NPh (*para*)), 47.0 (d, $^2J_{P-C}$ = 5 Hz, NCH_2Me), 13.8 (d, $^3J_{P-C}$ = 5 Hz, NCH_2Me) 13.5 (Cp*). Anal. Found: C, 61.65; H, 7.16; N, 8.74. Calcd: C, 61.92; H, 6.88; N, 8.50.

Syntheses of Cp′$TiMe_2(NP(NR_2)_3)$ (Cp′ = Cp, R = Me 27,[79] Et 28, Pr 29, Bu 30, R_2 = *i*-PrMe 31, EtPh 32; Cp′ = Cp*, R = Me 33, Et 34, Pr 35, Bu 36, R_2 = *i*-PrMe 37, EtPh 38). These compounds were prepared in a similar manner, and thus only one synthesis is detailed. To a yellow slurry of $CpTiCl_2(NP(NMe_2)_3)$ (0.201 g, 0.557 mmol) in ether (10 mL) was added 1.4 M MeLi in ether (0.83 mL, 1.162 mmol). The solvent was removed immediately under vacuum to produce a green residue. The green residue was extracted with hexanes (10 mL), and the LiCl was removed by filtration. The solvent was removed under vacuum to produce a green residue. **27**: Yield 0.152 g, 0.475 mmol, 85%. $^{31}P\{^1H\}$ NMR: δ 1.5. ^1H NMR: δ 6.22 (s, 5H, Cp), 2.40 (d, 18H, $^3J_{P-H}$ = 10 Hz, NMe), 0.77 (s, 6H, TiMe). $^{13}C\{^1H\}$ NMR: δ 111.2 (Cp), 41.2 (TiMe), 37.4 (d, $^2J_{P-C}$ = 3 Hz, NMe). Anal. Found: C, 47.54; H, 9.09; N, 17.85. Calcd: C, 48.76; H, 9.13; N, 17.50. **28**: Yield 0.198 g, 0.490 mmol, 99%. $^{31}P\{^1H\}$ NMR: δ −1.0. ^1H NMR: δ 6.22 (s, 5H, Cp), 2.98 (dq, 12H, $^3J_{P-H}$ = 10 Hz, $^3J_{H-H}$ = 7 Hz, NCH_2Me), 0.97 (t, 18H, $^3J_{H-H}$ = 7 Hz, CH_2Me), 0.65 (s, 6H, TiMe). $^{13}C\{^1H\}$ NMR: δ 111.1 (Cp), 40.9 (TiMe), 39.9 (d, $^2J_{P-C}$ = 4 Hz, NCH_2), 14.5 (s, CH_2Me). Anal. Found: C, 55.69; H, 10.03; N, 13.53. Calcd: C, 56.43; H, 10.22; N, 13.85. **29**: Yield: 0.130 g, 0.266 mmol, 87%. $^{31}P\{^1H\}$ NMR: δ −0.6. ^1H NMR: δ 6.27 (s, 5H, Cp), 2.97 (m, 12H, NCH_2CH_2Me), 1.53 (m, 12H, NCH_2CH_2Me), 0.82 (t, 18H, $^3J_{H-H}$ = 7 Hz, CH_2Me), 0.71 (s, 6H, TiMe). $^{13}C\{^1H\}$ NMR: δ 111.2 (Cp), 48.9 (d, $^2J_{P-C}$ = 4 Hz, NCH_2CH_2), 41.1 (s, TiMe), 22.7 (d, $^3J_{P-C}$ = 3 Hz, NCH_2CH_2Me), 12.1 (s, CH_2Me). Anal. Found: C, 60.58; H, 11.27; N 11.28. Calcd: C, 61.46; H, 10.93; N, 11.47. **30**: Yield: 0.198 g, 0.346 mmol, 76%. $^{31}P\{^1H\}$ NMR: δ 0.0. ^1H NMR: δ 6.30 (s, 5H, Cp), 3.12 (m, 12H, NCH_2CH_2), 1.61 (m, 12H, $NCH_2CH_2CH_2$), 1.27 (pseudo sextet, 12H, $^3J_{H-H}$ = 7 Hz, CH_2Me), 0.94 (t, 18H, $^3J_{H-H}$ = 7 Hz, CH_2Me), 0.72 (s, 6H, TiMe). $^{13}C\{^1H\}$ NMR: δ 111.2 (Cp), 46.9 (d, $^2J_{P-C}$ = 4 Hz, NCH_2CH_2), 41.2 (TiMe), 31.8 (d, $^3J_{P-C}$ = 3 Hz, $NCH_2CH_2CH_2$), 21.4 (s, CH_2Me), 14.7 CH_2Me). Anal. Found: C, 63.98; H, 10.83; N, 10.72. Calcd: C, 65.01; H, 11.44; N, 9.78. **31**: Yield: 0.175 g, 0.433 mmol, 93%. $^{31}P\{^1H\}$ NMR: δ −1.0. ^1H NMR: δ 6.21 (s, 5H, Cp), 4.27 (d(sept), 3H, $^3J_{P-H}$ = 10 Hz,$^3J_{H-H}$ = 7 Hz $CHMe_2$), 2.21 (d, 9H, $^3J_{P-H}$ = 10 Hz, NMe), 1.01 (d, 18H, $^3J_{H-H}$ = 7 Hz, $CHMe_2$), 0.64 (s, 6H, TiMe). $^{13}C\{^1H\}$ NMR: δ 111.1 (Cp), 46.5 (d, $^2J_{P-C}$ = 5 Hz, $CHMe_2$), 40.8 (TiMe), 26.6 (d, $^2J_{P-C}$ = 3 Hz, NMe), 20.7 (d, $^3J_{P-C}$ = 3 Hz, $CHMe_2$). Anal. Found: C, 55.48; H, 10.34; N, 14.21. Calcd: C, 56.43; H, 10.22; N, 13.85. **32**: Yield: 0.196 g, 0.357 mmol, 99%. $^{31}P\{^1H\}$ NMR: δ −16.1. ^1H NMR: δ 7.24 (d, 6H, $^3J_{H-H}$ = 8 Hz, NPh (*ortho*)), 7.14 (pseudo t, 6H, $^3J_{H-H}$ = 8 Hz, NPh (*meta*)), 6.98 (t, 3H, $^3J_{H-H}$ = 7 Hz, NPh (*para*)), 5.85 (s, 5H, Cp), 3.47 (dq, 6H, $^3J_{P-H}$ = 7 Hz, $^3J_{H-H}$ = 7 Hz, NCH_2Me), 0.77 (t, 9H, $^3J_{H-H}$ = 7 Hz, NCH_2Me), 0.66 (s, 6H, TiMe). $^{13}C\{^1H\}$ NMR: δ 143.8 (d, $^2J_{P-C}$ = 4 Hz, NPh (*ipso*)), 131.2 (d, $^3J_{P-C}$ = 3 Hz, NPh (*ortho*)), 129.3 (NPh (*meta*)), 126.3 (NPh (*para*)), 111.7 (Cp), 46.5 (d, $^2J_{P-C}$ = 4 Hz, NCH_2Me), 43.7 (TiMe), 14.4 (CH_2Me). Anal. Found: C, 68.03, H, 7.42; N, 9.94. Calcd: C, 67.88; H, 7.53; N, 10.21. **33**: Yield: 0.171 g, 0.438 mmol, 90%. $^{31}P\{^1H\}$ NMR: δ 0.4. ^1H NMR: δ 2.50 (d, 18H, $^3J_{P-H}$ = 10 Hz, NMe_2), 2.08 (s, 15H, Cp*), 0.49 (s, 6H, $TiMe_2$). $^{13}C\{^1H\}$ NMR: δ 119.0 (Cp*), 43.1 (TiMe), 37.7 (d, $^2J_{P-C}$ = 4 Hz, NMe_2), 12.6 (Cp*). Anal. Found: C, 55.17; H, 10.16; N, 14.59. Calcd: C, 55.38; H, 10.07; N, 14.35. **34**: Yield: 0.180 g,

Table 1. Calculated Solution Phase Relative Energies[a] (kcal/mol) for the Mechanism Depicted in Figure 1

R	1′	2′	3′	4′	TS1	5′	6′	7′	8′	TS2	9′
Me	0	−23.7	17.3	0	6.4	−9.1	−12.8	−42.2	−21.3	−18.5	−35.5
NH_2	0	−22.9	17.7	0	6.6	−9.0	−12.8	−44.9	−22.5	−19.2	−35.8
H[b]	0	−19.1	25.4	6.5	12.5	-2.9	-5.8	−37.2	−15.9	−13.2	−30.0
	0	*−14.3*	*74.8*	*53.4*	*60.2*	*44.9*	*41.8*	*−34.4*	*28.0*	*31.2*	*15.1*
Cl	0	−5.9	42.5	22.1	27.2	12.2	9.9	−27.4	0.0	0.4	−16.1
F	0	−5.6	40.5	19.8	24.5	9.6	7.4	−27.2	−2.6	−2.3	−18.8

[a] B3LYP/BS2//B3LYP/LANL2DZ COSMO. Solvent toluene (ϵ = 2.379). [b] Italicized numbers refer to B3LYP/BS2//B3LYP/LANL2DZ gas phase relative energies.

0.379 mmol, 93%. $^{31}P\{^1H\}$ NMR: δ −0.9. ^1H NMR: δ 3.11 (dq, 12H, $^3J_{P-H}$ = 10 Hz, $^3J_{H-H}$ = 7 Hz, NCH_2Me), 2.08 (s, 15H, Cp*), 1.00 (t, 18H, $^3J_{H-H}$ = 7 Hz, CH_2Me), 0.43 (s, 6H, TiMe). $^{13}C\{^1H\}$ NMR: δ 118.7 (Cp*), 43.2 (TiMe), 39.7 (d, $^2J_{P-C}$ = 4 Hz, NCH_2Me), 14.4 (CH_2Me), 12.5 (Cp*). Anal. Found: C, 60.00; H, 10.89; N, 11.55. Calcd: C, 60.75; H, 10.83; N, 11.81. **35**: Yield: 0.163 g, 0.272 mmol, 83%. $^{31}P\{^1H\}$ NMR: δ −1.0.^1H NMR: δ 3.10 (m, 12H, NCH_2CH_2), 2.10 (s, 15H, Cp*), 1.55 (m, 12H, NCH_2CH_2), 0.85 (t, 18H, $^3J_{H-H}$ = 7 Hz, CH_2Me), 0.45 (s, 6H, TiMe). $^{13}C\{^1H\}$ NMR: δ 118.4 (Cp*), 48.2 NCH_2), 42.9 (TiMe), 21.8 (NCH_2CH_2Me), 12.2 (Cp*), 11.8 (CH_2Me). Anal. Found: C, 64.74; H, 11.53; N, 9.83. Calcd: C, 64.49; H, 11.37; N, 10.03. **36**: Yield: 0.118 g, 0.173 mmol, 90%. $^{31}P\{^1H\}$ NMR: δ −0.7. ^1H NMR: δ 3.23 (m, 12H, NCH_2), 2.12 (s, 15H, Cp*), 1.63 (m, 12H, $NCH_2CH_2CH_2$), 1.30 (m, 12H, CH_2Me), 0.95 (t, 18H, $^3J_{H-H}$ = 7 Hz, CH_2Me), 0.45 (s, 6H, TiMe). $^{13}C\{^1H\}$ NMR: δ 118.4 (Cp*), 46.2 (NCH_2), 43.0 (TiMe), 31.4 (d, $^3J_{P-C}$ = 3 Hz, $NCH_2CH_2CH_2$), 21.1 CH_2Me), 14.4 (s, CH_2Me), 12.2 (Cp*). Anal. Found: C, 66.58; H, 11.60; N, 8.34. Calcd: C, 67.26; H, 11.76; N, 8.72. **37**: Yield: 0.171 g, 0.360 mmol, 93%. $^{31}P\{^1H\}$ NMR: δ −1.7. ^1H NMR: δ 4.31 (d(sept), 3H, $^3J_{P-H}$ = 10 Hz,$^3J_{H-H}$ = 7 Hz $CHMe_2$), 2.32 (d, 9H, $^3J_{P-H}$ = 10 Hz, NMe), 2.07 (s, 15H, Cp*), 1.05 (d, 18H, $^3J_{H-H}$ = 7 Hz, $CHMe_2$), 0.41 (s, 6H, TiMe). $^{13}C\{^1H\}$ NMR: δ 118.8 (Cp*), 46.2 (d, $^2J_{P-C}$ = 6 Hz, $CHMe_2$), 43.0 (TiMe), 27.0 (d, $^2J_{P-C}$ = 3 Hz, NMe), 20.9 (d, $^3J_{P-C}$ = 3 Hz, $CHMe_2$), 12.5 (Cp*). Anal. Found: C, 60.70; H, 11.12; N, 11.59. Calcd: C, 60.75; H, 10.83; N, 11.81. **38**: Yield: 0.163 g, 0.263 mmol, 88%. $^{31}P\{^1H\}$ NMR: δ −13.4. ^1H NMR: δ 7.21 (d, 6H, $^3J_{H-H}$ = 7 Hz NPh (*ortho*)), 7.13 (pseudo t, 6H, $^3J_{H-H}$ = 7, NPh (*meta*)), 6.97 (t, 3H, $^3J_{H-H}$ = 7 Hz, NPh (*para*)), 3.65 (dq, 6H, $^3J_{P-H}$ = 7 Hz, $^3J_{H-H}$ = 7 Hz, NCH_2Me), 1.97 (s, 15H, Cp*), 0.71 (t, 9H, $^3J_{H-H}$ = 7 Hz, NCH_2Me), 0.55 (s, 6H, TiMe). $^{13}C\{^1H\}$ NMR: δ 144.1 (NPh (*ipso*)), 130.0 (NPh), 129.2 (NPh), 125.9 (NPh), 119.6 (Cp*), 46.5 (NCH_2Me), 45.9 (TiMe), 14.2 (NCH_2Me), 12.5 (Cp*). Anal. Found: C, 69.45, H, 8.48; N, 9.08. Calcd: C, 69.89; H, 8.31; N, 9.06.

Polymerization Protocol. Purification of reagents used in the polymerizations was similar to that described above. Polymerization experiments were performed using a Büchi polymerization reactor. In all polymerizations, 600 mL of toluene was transferred into the reactor, heated to 30 ± 2 °C, and presaturated with ethylene prior to injection of precatalyst and cocatalyst. The solution was stirred at 1000 rpm for the duration of the polymerization experiment. At the end of the experiments, the contents of the reactor were emptied into a 4 L beaker containing approximately 200 mL of 10% HCl (v/v) in MeOH. The polymer that precipitated was collected by filtration, washed with water and acetone, and dried to a constant weight. Polymerization experiments using MAO as the cocatalyst were conducted for 30 min. In these polymerizations, 500 equiv of MAO was injected into the reactor and the solution was stirred for 5 min prior to injecting a toluene solution of the titanium dichloride precatalyst. Polymerization experiments using $B(C_6F_5)_3$ as the cocatalyst were conducted for 10 min. In these experiments, 20 equiv of triisobutylaluminum hydride (T*i*BAl) was injected into the reactor and the solution was stirred for 5 min prior to injecting toluene solutions of the titanium dimethyl precatalyst and the $B(C_6F_5)_3$ cocatalyst.

X-ray Data Collection and Reduction. Crystals were manipulated and mounted in capillaries in a glovebox, thus maintaining a dry, O_2-free environment for each crystal. Diffraction experiments were performed on a Siemens SMART System CCD diffractometer. The data were collected in a hemisphere of data in 1329 frames with 10 s exposure times. The observed extinctions were consistent with the space groups in each case. The data sets were collected (4.5° < 2θ < 45−50.0°). A measure of decay was obtained by re-collecting the first 50 frames of each data set. The intensities of reflections within these frames showed no statistically significant change over the duration of the data collections. The data were processed using the SAINT and XPREP processing packages. An empirical absorption correction based on redundant data was applied to each data set. Subsequent solution and refinement was performed using the SHELXTL solution package operating on a Pentium computer.

Structure Solution and Refinement. Non-hydrogen atomic scattering factors were taken from the literature tabulations.[82] The heavy atom positions were determined using direct methods employing the SHELXTL direct methods routine. The remaining non-hydrogen atoms were located from successive difference Fourier map calculations. The refinements were carried out by using full-matrix least-squares techniques on *F*, minimizing the function $w(|F_o| - |F_c|)^2$ where the weight *w* is defined as $4F_o^2/2\sigma(F_o^2)$ and F_o and F_c are the observed and calculated structure factor amplitudes. In the final cycles of each refinement, all non-hydrogen atoms were assigned anisotropic temperature factors in the absence of disorder or insufficient data. In the latter cases atoms were treated isotropically. C−H atom positions were calculated and allowed to ride on the carbon to which they are bonded assuming a C−H bond length of 0.95 Å. H atom temperature factors were fixed at 1.10 times the isotropic temperature factor of the C atom to which they are bonded. The H atom contributions were calculated, but not refined. The locations of the largest peaks in the final difference Fourier map calculation as well as the magnitude of the residual electron densities in each case were of no chemical significance. Addition details are provided Table 4 and in the Supporting Information.

Computational Chemistry. Molecular mechanics calculations were conducted using the MM3 force field as implemented in CAChe 6.0 for windows developed by CAChe Group, Fujitsu. All DFT calculations were performed using the Gaussian 98 suite of programs.[83] Optimized gas phase geom-

(82) Cromer, D. T.; Mann, J. B. *Acta Crystallogr. A* **1968**, *A24*, 321−324.

(83) Frisch, M. J.; Trucks, G. W.; Schlegel, H. B.; Scuseria, G. E.; Robb, M. A.; Cheeseman, J. R.; Zakrzewski, V. G.; Montgomery, J. A.; Stratmann, R. E.; Burant, J. C.; Dapprich, S.; Millam, J. M.; Daniels, A. D.; Kudin, K. N.; Strain, M. C.; Farkas, O.; Tomasi, J.; Barone, V.; Cossi, M.; Cammi, R.; Mennucci, B.; Pomelli, C.; Adamo, C.; Clifford, S.; Ochterski, J.; Petersson, G. A.; Ayala, P. Y.; Cui, Q.; Morokuma, K.; Malick, D. K.; Rabuck, A. D.; Raghavachari, K.; Foresman, J. B.; Cioslowski, J.; Ortiz, J. V.; Stefanov, B. B.; Liu, G.; Liashenko, A.; Piskorz, P.; Komaromi, I.; Gomperts, R.; Martin, R. L.; Fox, D. J.; Keith, T.; Al-Laham, M. A.; Peng, C. Y.; Nanayakkara, A.; Gonzalez, C.; Challacombe, M.; Gill, P. M. W.; Johnson, B. G.; Chen, W.; Wong, M. W.; Andres, J. L.; Head-Gordon, M.; Replogle, E. S.; Pople, J. A. *Gaussian 98 (Revision A.7)*; Gaussian, Inc.: Pittsburgh, PA, 1998.

Table 2. Calculated Energies for $[CpTiR'(NPR_3)]^+$ (R′ = Me, Pr)[a]

R	E_{ipf}[b]	E_{ips}[c]	E_{C-Me}[d]	E_{ib-Me}[e]	E_{ips-Pr}[f]	E_{C-Pr}[g]	E_{ib-Pr}[h]
Me	−23.7	41.1	−17.4	6.4	29.4	−8.6	2.8
NH_2	−22.9	40.6	−17.7	6.6	32.1	−9.8	3.4
H[i]	−19.1	44.6	−18.9	5.9	31.4	−10.1	2.8
	−14.3	89.1	−21.4	6.8	76.2	−11.0	3.2
Cl	−5.9	48.4	−20.4	5.1	37.3	−9.9	0.4
F	−5.6	46.1	−20.8	4.8	34.6	−10.0	0.3

[a] B3LYP/BS2//B3LYP/LANL2DZ COSMO. Solvent toluene (ϵ = 2.379). [b] Ion-pair formation energy, corresponding to **1′** + BCl_3 → **2′** + E_{ipf}. [c] Me-cation/anion separation energy, corresponding to **2′** → **3′**+ $[MeBCl_3]^-$ +E_{ips-Me}. [d] Me-cation-C_2H_4 binding, corresponding to **3′** + C_2H_4 → **4′** + E_{C-Me}. [e] Insertion barrier (Me-cation), corresponding to **4′** → **TS1** + E_{ib-Me}. [f] Pr-cation/anion separation energy, corresponding to **7′** → **6′** + $[MeBCl_3]^-$ + E_{ips-Pr}. [g] Pr−cation-C_2H_4 binding energy, corresponding to **6′** + C_2H_4 → **8′** + E_{C-Pr}. [h] Insertion barrier (Pr-cation), corresponding to **8′** → **TS2** + E_{ib-Pr}. [i] Italicized numbers refer to B3LYP/BS2//B3LYP/LANL2DZ gas phase values.

Table 3. Calculated Atomic Charges on Ti[a]

R	$CpTiMe_2NPR_3$	$[CpTiMeNPR_3]^+$
Me	0.78	0.90
NH_2	0.79	0.91
H	0.84	0.96
Cl	0.94	1.05
F	0.91	1.05

[a] Mulliken Charges from B3LYP/BS2//B3LYP/LANL2DZ. COSMO solvent toluene (ϵ = 2.379) calculations.

etries were obtained using the Becke3 exchange functional,[84] as implemented in Gaussian 98,[85] in combination with the Lee, Yang, and Parr correlation functional,[86] i.e., the B3LYP method. The LANL2DZ basis set was used for geometry optimizations and energy calculations. Relative energies were obtained by performing single-point calculations at the B3LYP/BS2 level of theory, based on the above geometries. The BS2 basis set is a larger basis set consisting of the 6-31G(d,p) basis set[87−90] for H, B, C, N, and F atoms, and the LANL2DZ basis sets for Ti, Ni, P, and Cl. As previously recommended by Torrent, Solà, and Frenking,[91] for Ti, the LANL2DZ basis set was supplemented with a set of (*n*)p functions for transition metals developed by Couty and Hall.[92] In addition, for P, a d function with an exponent of 0.34 was added.[93] This basis set is expected to provide more reliable relative energies than the smaller LANL2DZ basis set. Solvent effects were approximated with single-point calculations using B3LYP/BS2 on gas phase B3LYP/LANL2DZ geometries using the COSMO method[94] with the dielectric constant of ϵ = 2.379 for toluene. Toluene was chosen since all polymerization experiments reported herein used toluene as the solvent. The nature of transition structures was confirmed by calculating the harmonic vibrational frequencies. Relaxed potential energy scans along the C−C bond distances that served as the reaction coordinates, followed by full geometry optimizations, were used to confirm that all transition states were connected backward to the

Table 4. Crystallographic Data[a]

	6	**7**	**15**	**19**	**21**	**22**	**24**	**25**
formula	$C_{24}H_{30}N_3P$	$C_{27}H_{24}N_3P$	$C_{11}H_{23}Cl_2N_4PTi$	$C_{17}H_{35}Cl_2N_4PTi$	$C_{16}H_{33}Cl_2N_4PTi$	$C_{22}H_{45}Cl_2N_4PTi$	$C_{34}H_{69}Cl_2N_4PTi$	$C_{22}H_{45}Cl_2N_4PTi$
fw	391.48	421.47	361.10	445.26	431.23	515.39	683.70	515.39
a (Å)	13.088(8)	18.76(1)	8.650(1)	17.752(9)	12.847(7)	10.69(2)	10.685(6)	16.129(9)
b (Å)	22.65(2)		11.349(3)	16.426(8)	12.747(7)	16.14(2)	22.70(1)	8.836(5)
c (Å)	14.672(8)	11.190(8)	18.049(3)	18.85(1)	14.182(7)	17.46(3)	18.230(9)	20.81(1)
γ (deg)	90.121(13)		97.38(1)	116.24(1)	102.778(9)	107.76(2)	106.67(1)	91.76(1)
crystal syst	monoclinic	trigonal	monoclinic	monoclinic	monoclinic	monoclinic	monoclinic	monoclinic
V (Å^3)	4350(5)	3411(4)	1757.1(6)	4931(4)	2265(2)	2867(7)	4235(4)	2965(3)
space group	*Cc*	*R*3*c*	$P2_1/n$	$P2_1/c$	$P2_1/n$	$P2_1/n$	*Cc*	$P2_1/c$
d(calc) (g cm^{-1})	1.196	1.231	1.365	1.200	1.265	1.194	1.072	1.155
Z	8	6	4	8	4	4	4	4
abs coeff, μ (cm^{-1})	0.140	0.140	0.875	0.636	0.690	0.556	0.391	0.538
no. of data collected	9174	4550	3044	20764	9429	12 093	8986	12 225
no. of data with $F_o^2 > 3\sigma(F_o^2)$	4395	1086	2659	7032	3240	4083	4870	4199
no. of variables	505	94	172	451	217	271	379	271
R	0.0580	0.0487	0.0543	0.0515	0.0402	0.0583	0.0326	0.0407
R_w	0.1559	0.0982	0.1457	0.1327	0.1170	0.1306	0.0714	0.1144
GOF	1.054	1.006	1.048	0.924	1.044	0.919	0.854	0.989

[a] Data were collected at 20 °C with Mo Kα radiation (λ = 0.71069 Å); $R = \sum|F_o| - |F_c|/\sum|F_o|$, $R_w = [\sum(|F_o| - |F_c|)^2/\sum|F_o|^2]^{0.5}$.

(84) Becke, A. D. *Phys. Rev. A* **1988**, *38*, 3098−3100.
(85) Stephens, P. J.; Devlin, F. J.; Chabalowski, C. F.; Frisch, M. J. *J. Phys. Chem.* **1994**, *98*, 11623−11627.
(86) Lee, C.; Yang, W.; Parr, R. G. *Phys. Rev. B: Condensed Matter Mater. Phys.* **1988**, *37*, 785−789.
(87) Ditchfield, R.; Hehre, W. J.; Pople, J. A. *J. Chem. Phys.* **1971**, *54*, 724−728.
(88) Hehre, W. J.; Ditchfield, R.; Pople, J. A. *J. Chem. Phys.* **1972**, *56*, 2257−2261.
(89) Hariharan, P. C.; Pople, J. A. *Theor. Chim. Acta* **1973**, *28*, 213−222.
(90) Hariharan, P. C.; Pople, J. A. *Mol. Phys.* **1974**, *27*, 209−214.
(91) Torrent, M.; Sola, M.; Frenking, G. *Chem. Rev.* **2000**, *100*, 439−493.
(92) Couty, M.; Hall, M. B. *J. Comput. Chem.* **1996**, *17*, 1359−1370.
(93) Feldgus, S.; Landis, C. R. *Organometallics* **2001**, *20*, 2374−2386.
(94) Barone, V.; Cossi, M. *J. Phys. Chem. A* **1998**, *102*, 1995−2001.

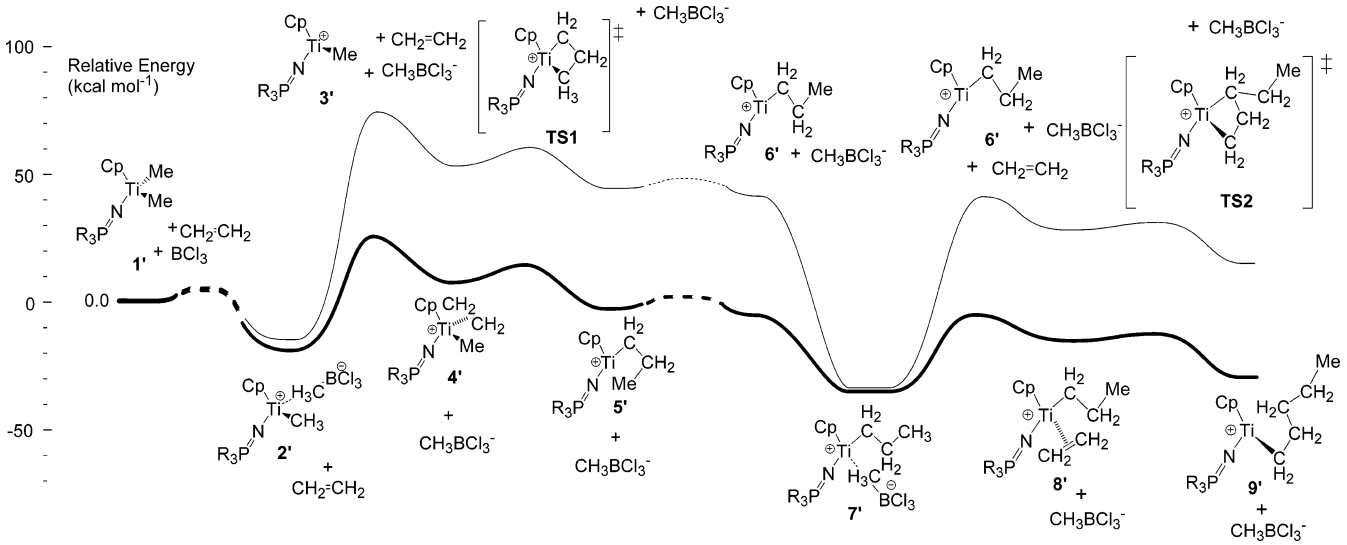

Figure 1. Generalized mechanism and energy profile for two consecutive solution phase (bold) and gas phase (thin line) insertion reactions.

reactants and forward to the products. Atomic charges on titanium reported herein are Mulliken charges from the B3LYP/BS2 COSMO single-point calculations (Table 3). All relative energies are reported in kcal mol^{-1}, bond lengths in angstroms (Å), and angles in degrees (°), unless otherwise noted.

Results and Discussion

Polymerization Mechanism. Our strategy to catalyst design began with a computational examination of the mechanism of the first two insertions of ethylene polymerization using the model precursor $CpTiMe_2$-NPH_3 and the Lewis acid BCl_3. Ziegler and co-workers have previously described similar computations for the first insertion of ethylene for $CpTiMe_2(NPR_3)$, where R = H, Me, *t*-Bu, employing $B(C_6F_5)_3$ as a Lewis acid.[58,59] The mechanism begins with the formation of an ion pair $[CpTiMe(NPH_3)][MeBCl_3]$, **2′**, lying 19.1 kcal mol^{-1} lower in energy. The transition state structure for this reaction was not located due to the rather soft potential surface; nonetheless, experimental data has confirmed the formation and identity of the zwitterionic species $[CpTiMe(NPt\text{-}Bu_3)][MeB(C_6F_5)l_3]$.[41] In addition, the experimental barrier for formation of the related ion pair $[(1,2\text{-}Me_2Cp)_2ZrMe][MeB(C_6F_5)_3]$ was estimated by Marks and co-workers to be approximately 3 kcal mol^{-1}.[95] Separation of the ion pair $[CpTiMe(NPH_3)][MeBCl_3]$, **2′**, to discrete ions was calculated to require 44.6 kcal mol^{-1} of energy in the solution phase. Subsequent steps considered separated cations, although studies of counterion effects by Marks et al.[57] have inferred that this approach overestimates energy barriers. The initial interaction of the cation with ethylene results in the formation of an energetically favorable ethylene π-complex, 18.9 kcal mol^{-1} lower in energy, which agrees well with the complexation energy previously reported by Ziegler and co-workers (−20.1 kcal mol^{-1}, gas phase).[59] Insertion of ethylene into the Ti−Me bond proceeds via a metallacycle transition state and results in the formation of a propyl cation with a γ-agostic interaction with a barrier of just 5.9 kcal mol^{-1}. Rearrangement to the β-agostic propyl cation is thermodynamically favored. Prior studies of the polymerization mechanism for constrained geometry and metallocene catalysts suggested such conversions from γ- to β-agostic conformations are facile.[61,71,96] Re-coordination of the $[MeBCl_3]^-$ counterion to form the thermodynamically favored ion pair $[CpTiPr(NPH_3)][MeBCl_3]$, **7′** (31.4 kcal mol^{-1} lower in energy), represented both the conclusion of the first insertion of ethylene and the starting point for the subsequent ethylene insertion step. Consideration of the solvent effects[48,49,51,56−58,69] for toluene using the COSMO[94,97] method revealed that the slightly polar solvent generally stabilizes all ions and ionic complexes, as expected. This solvent correction significantly reduces the magnitude of the ion pair separation and ethylene binding energies and increases the magnitude of the ion pair formation energy for the phosphinimide-complex reaction sequence (Figure 1, Table 1). Similar trends have been previously observed.[57,59]

Calculations for a second ethylene insertion followed a similar reaction coordinate with lower solvent phase and gas phase energy profiles (Figure 1). These results are also consistent with computational studies of ethylene insertion barrier into $[Cp_2ZrR]^+$,[67] $[[H_2Si(C_5H_4)$-$(t\text{-}BuN)]TiR]^+$,[57] and $[(CpSiH_2NH)TiR]^+$ [71] (R = Me, Pr). As observed for the first insertion, the largest barrier to the second insertion occurs for the ion pair dissociation. Subsequent reaction of the separated β-agostic propyl cation $[CpTiPr(NPH_3)]^+$, **6′,** with C_2H_4 proceeds to give the ethylene π-complex, which is 10.1 kcal mol^{-1} lower in energy. In the final step, ethylene insertion into the Ti−Pr bond requires only 2.7 kcal mol^{-1} of energy to give a γ-agostic pentyl cation, which is an additional 14.1 kcal mol^{-1} lower in energy. Consistent with these computations, Landis et al. have previously shown that the first olefin insertion can be ca. 400 times slower than subsequent insertions for metallocene catalysts.[98]

(95) Deck, P. A.; Beswick, C. L.; Marks, T. J. *J. Am. Chem. Soc.* **1998**, *120*, 1772−1784.
(96) Lohrenz, J. C.; Woo, T. K.; T., Z. *J. Am. Chem. Soc.* **1995**, *117*, 12793−12800.
(97) Andzelm, J.; Kolmel, C.; Klamt, A. *J. Chem. Phys.* **1995**, *103*, 9312−9320.

Ligand Effects. Analogous calculations employing the model systems based on $CpTiMe_2(NPR_3)$, **1′**, (R = Me, NH_2, Cl, F), revealed that the atomic charges for the precursors and the cations $[CpTiMe(NPR_3)]^+$, **3′** (R = Me, NH_2, H, Cl, F), were consistent with the order of the electron-donating ability of the phosphinimides: Me ≅ NH_2 > H > Cl ≅ F. It is clear that, relative to H, electron-donating substituents (Me, NH_2) on the phosphinimide ligand produce lower relative energy profiles for the first and second ethylene insertions, while electron-withdrawing substituents afford higher energy profiles (Table 1). While the electronic properties of the phosphinimide ligand influence the ethylene complexation energies (E_{c-Me}, E_{c-Pr}) and the ethylene insertion barriers (E_{ib-Me}, E_{ib-Pr}) to a limited extent, the effects are small, with differences of only approximately 3 kcal mol^{-1} at most (Table 2).

In contrast, the magnitude of the ion pair formation energies follows the trend Me > NH_2 > H > Cl > F, with approximately an 18 kcal mol^{-1} difference between the most electron-rich titanium complex, $CpTiMe_2(NPMe_3)$, and the most electron-poor titanium complex, $CpTiMe_2(NPF_3)$ (Table 2). In related experimental work, Marks and co-workers showed that in reactions of the Lewis acids $B(C_6F_5)_2Ar$ (Ar = C_6F_5, 3,5-$F_2C_6H_3$, Ph, 3,5-$Me_2C_6H_3$) with $(1,2\text{-}Me_2Cp)_2ZrMe_2$ the ion pair formation energies and, thus, the extent to which the ion pair formed in equlibria, were qualitatively related to the polymerization activities.[95] In the present systems, if entropy contributions are assumed to be similar to those described by Marks et al., then electron-withdrawing substituents on the phosphinimide ligand would be expected to reduce the ability of cocatalysts to effect methyl abstraction, and thus reduce polymerization activity.

The ion pair separation energies for the methyl cations are also strongly affected by the electronic properties of the phosphinimide ligand, as electron-donating substituents result in reduced barriers to ion pair separation (Table 2). Such ligands should result in faster ethylene insertion. This view is in general agreement with the previous suggestions for other catalyst systems in which incorporation of electron-donating groups resulted in enhanced polymerization activities.[42,99−102]

The geometries of the propyl ion pairs **7′** (R = Me, NH_2, H) were minimized by introducing the $[MeBCl_3]^-$ counterion to the β-agostic propyl cation; however, for the F analogue it was not possible to ascertain an optimized geometry using this method. Instead, a Cl atom transfer from $[MeBCl_3]^-$ to titanium resulted in the formation of $CpTiPrCl(NPF_3)$ and $MeBCl_2$. A similar problem was reported by Lanza and co-workers during their investigations on constrained geometry catalysts.[49] To prevent the chloride atoms of $[MeBCl_3]^-$ from approaching the titanium, the Ti−C−B bond angle in

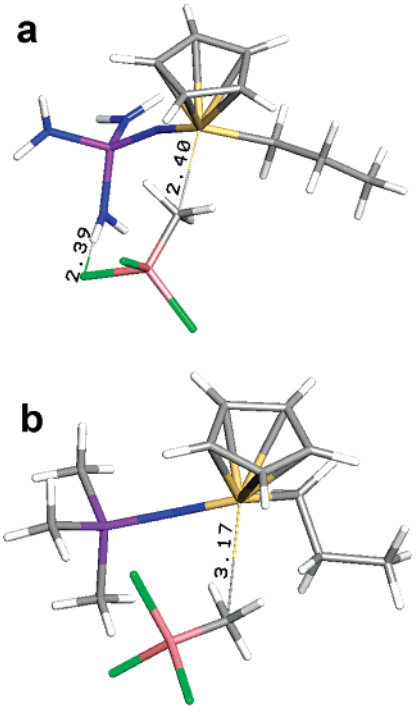

Figure 2. JIMP depictions[109] of propyl cation ion pairs for (a) R = NH_2 and (b) R = Me (H = white, B = pink, C = gray, N = blue, P = purple, Cl = green, Ti = yellow).

$[CpTiPr(NPF_3)][MeBCl_3]$ was constrained to 179.99°. Although this was also unsuccessful for the determination of a fully optimized structure, it did provide geometries in which the ion pair was bridged through the methyl group. Thus, for the subsequent B3LYP/BS2 COSMO calculations, the lowest energy geometry for the constrained model was employed. For the Cl-substituted model, $[CpTiPr(NPCl_3)][MeBCl_3]$, a separate problem was encountered, as a Cl atom from the ligand and the anion eliminated to form free Cl_2. Constraint of the B−Cl and P−Cl bond lengths resolved this problem and afforded a fully optimized geometry. In both cases, the use of constraints resulted in an underestimation of the ion pair separation. Nonetheless, it is clear that the electronic properties of the phosphinimide ligands result in a significant influence on the ion pair separation energies for the propyl cations (Table 2). It is interesting to note that for the propyl cation with R = NH_2 the ion pair separation energy is 32.1 kcal mol^{-1}, which is slightly more than the 29.4 kcal mol^{-1} for the R = Me analogue. This stands in contrast to that observed for the ion pair separation for the methyl cations, where the reverse is the case (R = NH_2: 40.6 kcal mol^{-1}; R = Me: 41.1 kcal mol^{-1}). This reversal may be due to the stronger binding of the anion in the propyl cation for R = NH_2 compared to the R = Me analogue, although N−H···Cl (2.39 Å) hydrogen bonding between the tris(amino)phosphinimide ligand and the anion may contribute to the stabilization energy of this ion pair (Figure 2).

The electronic properties of the phosphinimide ligand have little effect on the ethylene complexation energy for the propyl cations. On the other hand, complexes with electron-withdrawing groups Cl and F have insertion barriers that are 2−3 kcal mol^{-1} lower than for the corresponding electron-donating groups, Me (2.8 kcal mol^{-1}) and NH_2 (3.4 kcal mol^{-1}). This may be the result

(98) Landis, C. R.; Rosaaen, K. A.; Sillars, D. R. *J. Am. Chem. Soc.* **2003**, *125*, 1710−1711.
(99) Piccolrovazzi, N.; Pino, P.; Consiglio, G.; Sironi, A.; Moret, M. *Organometallics* **1990**, *9*, 3098−3105.
(100) Lee, I.-M.; Gauthier, W. J.; Ball, J. M.; Iyengar, B.; Collins, S. *Organometallics* **1992**, *11*, 2115−2122.
(101) Mohring, P. C.; Coville, N. J. *J. Organomet. Chem.* **1994**, *479*, 1−29.
(102) Klosin, J.; Kruper, W. J., Jr.; Nickias, P. N.; Roof, G. R.; De Waele, P.; Abboud, K. A. *Organometallics* **2001**, *20*, 2663−2665.

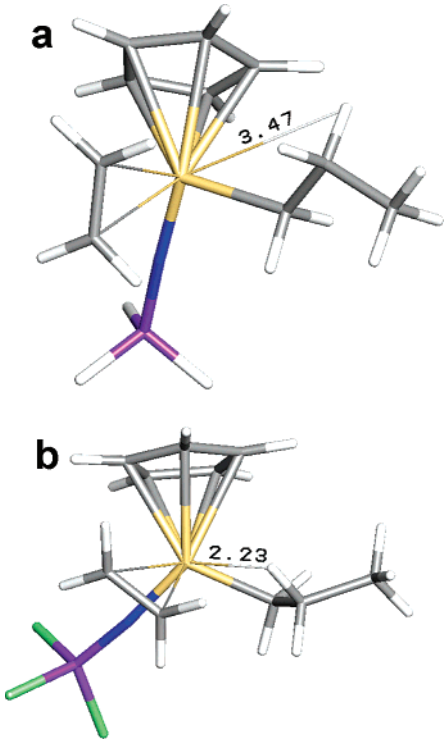

Figure 3. JIMP depictions[109] of propyl cation ethylene π-complexes for (a) R = H and (b) R = F (H = white, C = gray, N = blue, P = purple, F = green, Ti = yellow).

of β-agostic interactions that are present in the ethylene π-complexes for R = Cl or F, but absent for R = Me, NH_2, or H. Such β-agostic interactions may destabilize the ethylene π-complexes, thus decreasing the gap in energy between the π-complex and the transition state, and consequently lower the insertion barrier. In addition, the ethylene is bound in a conformation parallel to the Ti−N bond in the complexes with R = Me, NH_2, or H, while it is perpendicular to the Ti−N bond for R = Cl or F. The latter conformation is similar to the geometry of the transition state for ethylene insertion, thus facilitating insertion (Figure 3).

The present computational data suggest that increasing the electron-donating capability of the phosphinimide ligand reduces interactions between the titanium cation and anion, thus facilitiating ethylene coordination and increasing the rate of polymer progation. At the same time, electron-donating substituents increase the barrier from the ethylene π-complexes to the insertion transition state. However, the latter barrier is significantly smaller than the ion pair separation energy, and thus, in these catalyst systems, electron-donating groups enhance catalyst activity.

Synthetic Chemistry. The above computations suggest that amino and alkyl substituents on the phosphinimide ligand should facilitate ion separation and, thus, polymerization catalysis to a similar extent. Our previous experimental work has shown that while high-activity olefin polymerization catalysts can be derived from trialkylphosphinimide ligand complexes, the range of ligands that offer high activity is limited to those that are sterically demanding. From a synthetic perspective, the tris(amino)phosphine ligand precursors are much easier to prepare in high yield than sterically similar trialkylphosphines. In addition, since tris(amino)phosphines are derived from secondary amines and PCl_3, a

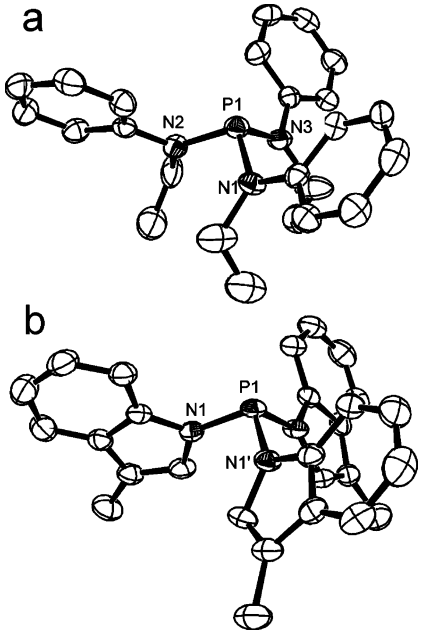

Figure 4. ORTEP drawings of (a) **6** and (b) **7**; 30% thermal ellipsoids are shown. Hydrogen atoms are omitted for clarity. **6**: P−N_{av} 1.725(4) Å, N−P−N_{av} 102.2(2)°. **7**: P−N 1.709(3) Å, N−P−N′ 100.60(13)°.

wide range of phosphinimide ligands are readily accessible from inexpensive starting materials. Thus, the tris(amino)phosphines $P(NMe_2)_3$, **1**, $P(NEt_2)_3$, **2**, and P(N(*n*-Pr)$_2$)$_3$, **3**, were obtained from commercial sources, while several other derivatives including P(N(*n*-Bu)$_2$)$_3$, **4**,[74] P(N*i*-PrMe)$_3$, **5**,[80] and $P(NEtPh)_3$, **6**,[81] were readily synthesized in moderate to good yields. In addition, P(*N*-3-methylindolyl)$_3$, **7**,[75] was prepared by generation of the lithium salt of 3-methylindole, followed by subsequent reaction with PCl_3. These species were spectroscopically characterized, and in the case of **6** and **7**, X-ray crystallographic studies confirmed the formulations. While the metric parameters were unexceptional, the solid state structures did reveal that the phenyl substituents on the nitrogen atoms of **6** and the indolyl arene rings of **7** were oriented in the same direction, i.e., canted up toward the "lone pair" on phosphorus (Figure 4).

Subsequent oxidation of these phosphines proceeds, in general, via standard methods.[103−105] Reaction of **1**−**6** with Me_3SiN_3 in refluxing toluene yielded the derivatives $Me_3SiNP(NR_2)_3$ (R = Me **8**, Et **9**, Pr **10**, Bu **11**; R_2 = *i*-PrMe **12**, EtPh **13**) as colorless oils in yields ranging from 68 to 95% (Scheme 2). These species were identified by multinuclear NMR spectroscopy. In contrast, attempts to synthesize Me_3SiNP(*N*-3-methylindolyl)$_3$, **14**, via treatment of **7** with Me_3SiN_3 while heating at refluxing temperature for an extended period of time (2 weeks), failed to effect oxidization of this phosphine, suggesting that steric congestion and the rigidity of the substituents precluded reaction. Experimental and theoretical data have previously supported the view that steric factors can alter the course of such Staudinger reactions.[106,107] Furthermore, P(*N*-3-methylindolyl)$_3$, **7**, previously displayed slow reactivity in other oxidation

(103) Staudinger, H.; Meyer, J. *Helv. Chim. Acta* **1919**, *2*, 635−646.
(104) Gololobov, Y. G.; Zhmurova, I. N.; Kasukhin, L. F. *Tetrahedron* **1981**, *37*, 437−472.
(105) Gololobov, Y. G.; Kasukhin, L. *Tetrahedron* **1992**, *48*, 1353−1406.

Table 5. Selected Metric Parameters from X-ray Structures

compd	Ti−Cl (Å)	Ti−N (Å)	N_{Ti}-P (Å)	Ti−N−P (deg)
15	2.298(2), 2.323(2)	1.759(3)	1.594(3)	164.3(2)
19	2.311(2), 2.309(2) 2.290(2), 2.298(2)	1.761(3), 1.769(4)	1.593(3) 1.592(4)	174.3(2) 173.1(3)
21	2.323(2), 2.310(1)	1.788(3)	1.589(3)	163.8(2)
22	2.317(3), 2.337(3)	1.786(4)	1.586(4)	175.7(2)
24	2.303(1), 2.313(2)	1.782(3)	1.592(3)	175.5(2)
25	2.311(1), 2.317(1)	1.778(2)	1.591(2)	170.3(2)

Scheme 2. Generalized Synthetic Route to Precatalysts

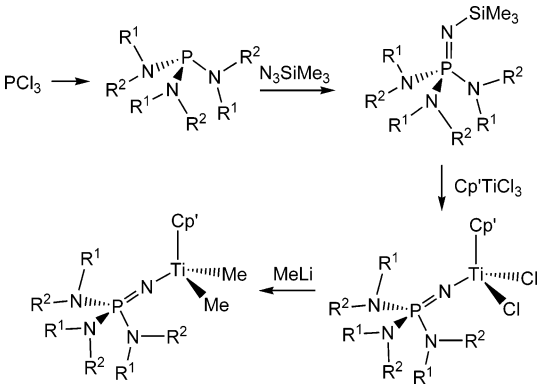

reactions, which was attributed to the poor electron-donating ability of phosphine resulting from the aromaticity *N*-3-methylindolyl substituents.[75]

The series of titanium complexes $Cp'TiCl_2(NP(NR_2)_3)$ (Cp′ = Cp, R = Me **15**, Et **16**, Pr **17**, Bu **18**, R_2 = *i*-PrMe **19**, EtPh **20**; Cp′ = Cp*, R = Me **21**, Et **22**, Pr **23**, Bu **24**, R_2 = *i*-PrMe **25**, EtPh **26**) were prepared by reaction of $Cp'TiCl_3$ and the corresponding phosphinimine $Me_3SiNP(NR_2)_3$. Generally the yields were good, ranging from 68 to 95%. Subsequent alkylation by MeLi or MeMgX (X = Cl, Br) afforded the corresponding Ti-dimethyl derivatives **27**−**38**, also in high yields of ca. 90% (Scheme 2). All complexes were characterized by elemental analysis and multinuclear NMR spectroscopy. In addition, X-ray crystallographic studies of **19**, **21**, **22**, **24**, and **25** are reported herein. It is worth mentioning that the structure of **15** has been previously reported.[108] Representative ORTEP depictions of these molecules are presented in Figure 5. The features of these compounds are typical of Ti-phosphinimide complexes (Table 5), with Ti−N distances of 1.759(3)−1.769(4) Å for the Cp derivatives and slightly longer (1.778(3)−1.788(3) Å) for the Cp* analogues. These variations are consistent with the greater electron-donating ability of the Cp* ligand. The Ti−N−P angles approach linearity, ranging from 163.8(2)° to 175.7(2)°.

Ethylene Polymerization. The complexes **15**, **16**, **19**−**22**, **25**, and **26** were tested for ethylene polymerization activity using 500 equiv of MAO as a cocatalyst. The polymerization experiments were conducted for 30 min, under an ethylene pressure of 2 atm, using catalyst concentrations of either 50 or 100 μmol L^{-1}. Toluene (600 mL) was used as the solvent, with a stir-rate of 1000 rpm. While **15**, **16**, **19**, **21**, **22**, and **25** resulted in low catalytic activity upon activation with MAO, the more sterically demanding phosphinimide ligand complexes afforded significantly higher activities (Table 6). For example, **20** and **26** exhibited higher catalyst activities of 150 and 200 g $mmol^{-1}$ h^{-1} atm^{-1}, respectively. These data are in agreement with the observations of related titanium trialkylphosphinimide complexes and suggest that enhanced steric bulk of the ligand has a positive effect on catalyst activity, possibly by slowing the rate of catalyst deactivation via attack at the phosphinimide-N atom.[37−39] The M_n values of the polyethylene derived under these conditions range from 39 to 257 000 (Table 6). The polydisperities range from 1.6 to 8.9 for these systems, suggesting that some side

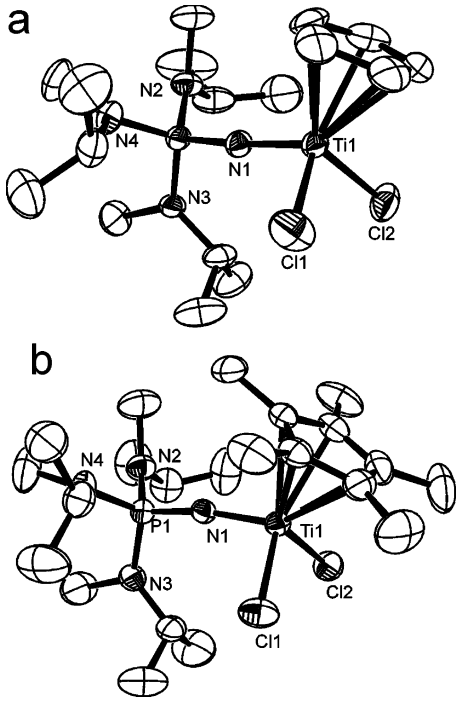

Figure 5. ORTEP drawings of (a) **19** and (b) **25**; 30% thermal ellipsoids are shown. Hydrogen atoms are omitted for clarity.

Table 6. Polymerization Testing of Precatalysts Using MAO as a Cocatalyst[a]

precatalyst	[cat] (μmol L^{-1})	PE yield (g)	activity (g $mmol^{-1}$ h^{-1} atm^{-1})	M_n	M_w	PDI
15	100	0.15	2.4	257 100	533 600	2.08
16	100	1.57	26	129 900	464 000	3.57
19	50	0.40	13	39 100	348 400	8.91
20	50	4.62	150	135 500	624 800	4.61
21	100	1.26	21	82 600	141 800	1.72
22	100	2.33	39	90 100	149 100	1.65
25	50	1.66	56	127 800	352 200	2.76
26	50	6.08	200	126 100	507 200	4.02

[a] Polymerization conditions: C_2H_4 P = 2 atm, T = 30 °C, solvent = 600 mL of toluene, stir rate = 1000 rpm, 500 equiv of MAO, reaction time = 30 min. Results of at least duplicate runs.

(106) Widauer, C.; Grutzmacher, H.; Shevchenko, I.; Gramlich, V. *Eur. J. Inorg. Chem.* **1999**, 1659−1664.
(107) Alajarin, M.; Conesa, C.; Rzepa, H. S. *J. Chem. Soc., Perkin Trans.* **1999**, 1811−1814.
(108) Von Haken Spence, R. E.; Stephan, D. W.; Brown, S. J.; Jeremic, D.; Wang, Q. (Nova Chemicals (International) S.A., Switz.) PCT Int. Appl.; WO, 2000, 38 pp.

Table 7. Polymerization Testing Using $B(C_6F_5)_3$ as a Cocatalyst[a]

	[cat] = 10		[cat] = 4				
precatalyst	activity	PE yield (g)	activity	PE yield (g)	M_n	M_w	PDI
27	350	0.70	2200	1.73	315 000	646 200	2.05
28	1800	3.53	3500	2.81	394 000	752 900	1.91
29			5500	4.37			
30			3600	2.88			
31	1900	3.79	3600	2.85	388 600	717 800	1.85
32	2600	5.30	4200	3.37	432 500	829 100	1.92
33	1200	2.44	4200	3.37	140 800	692 200	4.92
34	2000	4.06	4700	3.79	insoluble		
35			10000	8.33			
36			6100	4.88			
37	2100	4.25	4900	3.94	288 100	617 900	2.14
38	2300	4.54	4200	3.39	324 600	660 100	2.03
$Cp^*TiMe_2NPi\text{-}Pr_3$	1600	3.24	5200	4.17	493 400	1 012 000	2.05
$CpTiMe_2NPt\text{-}Bu_3$	2900	5.80	5600	4.50	437 800	786 300	1.80
Cp_2ZrMe_2	3500	6.93	16000	12.61	175 000	331 100	1.89

[a] Polymerization conditions: ethylene pressure = 2 atm, temperature = 30 °C, Solvent = 600 mL of toluene, stir rate = 1000 rpm, 2 equiv of $B(C_6F_5)_3$; 20 equiv of T*i*BAL, reaction time = 10 min. Results of at least duplicate runs. Activities are reported in the units g $mmol^{-1}$ h^{-1} atm^{-1}. [Cat] units: μmol/L.

reactions may provide access to variation in the active species. Similar observations have been previously reported for MAO activation of phosphinimide-based catalysts.[40−44]

The analogous methylated precatalysts **27**, **28**, **31**−**34**, **37**, and **38**, in concentrations of 10 μmol/L, were tested for ethylene polymerization activity using 2 equiv of $B(C_6F_5)_3$ as a cocatalyst and 20 equiv of T*i*BAl as the solvent purifier. These experiments were conducted for 10 min, under an ethylene pressure of 2 atm, using 600 mL of toluene as the solvent, and with a stir-rate of 1000 rpm. In contrast to the MAO activation strategy described above, all of these systems resulted in very high ethylene polymerization activity (1200−2600 g $mmol^{-1}$ h^{-1} atm^{-1}), although **27** exhibited polymerization activity that was somewhat lower (350 g $mmol^{-1}$ h^{-1} atm^{-1}) (Table 7). Among these catalysts, there appears to be a good correlation between the steric bulk of the ligands and the activity. For example, except for the analogues **31** and **38**, replacement of Cp with Cp* results in higher activity. Similarly, increased steric demands on the amino groups of the tris(amino)phosphinimide ligands also result in higher activity. The observation that increased electron-donating ligands (Cp* vs Cp) and increased steric bulk of the phosphinimide ligands yield higher catalyst activities is consistent with the dominant role for ion-pair separation energies in the polymerization energy profile.[58] Reduction of the catalyst concentrations to 4 μmol/L with conditions otherwise unchanged resulted in a further dramatic increase in the polymerization activities to the range 2200−10 000 g $mmol^{-1}$ h^{-1} atm^{-1} (Table 7). It should be noted that further reduction of the concentration of **38** to 2 μmol/L did not result in a further increase in polymerization activity, indicating that at 4 μmol/L diffusion-limited kinetics are no longer an issue. It is particularly noteworthy that among this family of highly active catalysts the precursor **36** exhibits activity that is almost twice as high as that achieved for the previously reported precatalysts derived from the trialkylphosphinimide complexes, $CpTiMe_2NP(t\text{-}Bu)_3$ and $Cp^*TiMe_2NP(t\text{-}Bu)_3$.[40,42] The M_n of the resulting polymers range from 140 000 to 433 000 (Table 7), while the polydispersities, in general less than 2.0, are consistent with single-site polymerization catalyst behavior.

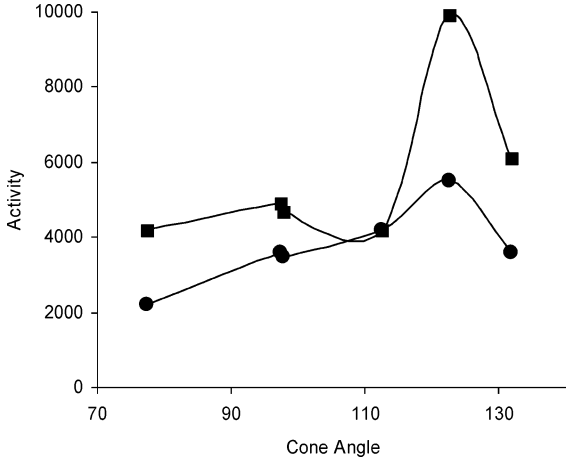

Figure 6. Plot of phosphinimide cone angle (deg) versus polymerization activity (g $mmol^{-1}$ h^{-1} atm^{-1}) for the catalysts derived from $CpTiMe_2(NPR_3)$ (●) and $Cp^*TiMe_2(NPR_3)$ (■).

Steric Effects. The steric bulk of the phosphinimide ligands can be expressed in terms of a "cone angle".[110] These angles, calculated by doubling the average of the three half-angles defined at titanium by the phosphorus atom and the outermost atom of the three substituents, were obtained both from crystallographic data and optimized models derived from molecular mechanics calculations (MM3) (Table 8). In the latter determinations, the Ti−N and P−N bond distances were fixed at values derived from X-ray data. In general, the cone angles computed in either fashion showed generally good agreement, with the exception of the values computed for $NP(Nn\text{-}Bu_2)_3$ (X-ray: 117.5°; MM3: 146.3°). This discrepancy was attributed to the flexibility of the long butyl chains and indicates that cone angles should be used only as a rough estimate of the steric size. Correlations of these cone angles with the polymerization activities showed qualitative relationships for both the Cp and Cp* series of tris(dialkylamino)phosphinimide-based catalysts (Figure 6). In the case of the tris(ethylphenylamino)phosphinimide ligand complexes,

(109) Manson, J.; Webster, C. E.; Hall, M. B. *JIMP Development*, Version 0.1 ed.; Texas A&M University: College Station, TX 77842.
(110) Tolman, C. A. *Chem. Rev.* **1977**, *77*, 313.

although the cone angle is calculated to be 112.5°, the activity of the derived catalyst is lower than those derived from $Cp^*TiMe_2NP(NEt_2)_3$ and $Cp^*TiMe_2NP(N\textit{i}\text{-}PrMe)_3$. This is attributed to the diminished electron-donating ability as a result of the presence of the aryl ring on nitrogen. In addition, this may be a reflection of the inherent error in the description of the steric bulk via an estimated cone angle.

Conclusions

The DFT calculations of the mechanism of polymerization for the series of catalyst models derived from $CpTiMe_2NPR_3$ (R = Me, NH_2, H, Cl, F) demonstrated the critical role of ion pairing in the determination of the overall barrier to polymerization, in agreement with other theoretical and experimental observations. The present study further suggests that ligand modifications that incorporate electron-donating substituents reduce this barrier and thus enhance polymerization activity. Based on these calculations and synthetic limitations, strategies to the readily accessible and easily varied family of compounds of general formula $Cp'TiX_2NP(NR_2)_3$ were developed. Activation of the dichloride derivatives with MAO revealed widely variable polymerization activities, an observation previously seen for phosphinimide-based catalysts. However, activation of the dimethyl analogues using B-based activators resulted in very high ethylene polymerization activities. In addition, for electronically similar tris(amino)phosphinimide ligands, polymerization activity was seen to increase with increasing steric bulk. Thus, in general, optimization of steric bulk and electronic characteristics to facilitate ion-pair separation and prolonged catalyst lifetime has been achieved, affording a readily accessible and easily varied family of highly active ethylene polymerization catalysts based on the tris(amino)phosphinimide ligand. Furthermore, this study effectively demonstrates the synergy of theoretical and experimental methods for the catalyst design. Further developments of this new class of single-site catalysts are the subject of ongoing efforts.

Table 8. Phosphinimide Cone Angles for $Cp^*TiCl_2(NPR_3)$ Complexes

NPR_3	cone angle (deg)	
R	MM3	X-ray[a]
R = NMe_2	77.5	77.2
R = NEt_2	94.7	100.9
R = N*n*-Pr_2	115.3	129.8[b]
R = N*n*-Bu_2	117.5	146.3
R = N*i*-PrMe	93.5	101.3
R = NEtPh	112.5	
R = *t*-Bu	87.2	84.2
R = *i*-Pr	75.7	81.3

[a] These values were derived from the X-ray reported herein. [b] Estimated from the X-ray data for **24**.

Acknowledgment. Financial support from NSERC of Canada, NOVA Chemicals Corporation, and the ORDCF is gratefully acknowledged. C.B. is grateful for the award of NSERC-IPGS and CCMR research scholarships. E.H. is grateful for the award of an OGS scholarship.

Supporting Information Available: Tables of calculated gas phase relative energies (kcal/mol) for the mechanism; gas phase ion-pair formation, ion-pair separation, and ethylene binding energies and insertion barriers for the methyl and propyl cations derived from $CpTiMe_2NPR_3$; and crystallographic information files (CIF). This material is available free of charge via the Internet at http://pubs.acs.org.

OM049545I